JOURNAL OF GEOPHYSICAL RESEARCH, VOL. 98, NO. A1, PAGES 13–32, JANUARY 1, 1993

Corotating MeV/amu Ion Enhancements at ≤1 AU From 1978 to 1986

I. G. RICHARDSON,[1] L. M. BARBIER, D. V. REAMES, AND T. T. VON ROSENVINGE

Laboratory for High Energy Astrophysics, NASA Goddard Space Flight Center, Greenbelt, Maryland

MeV/amu ion enhancements associated with corotating high-speed solar wind streams in 1978–1986 during pre–solar maximum to near solar minimum conditions are studied using ISEE 3/ICE, IMP 8, and Helios 1 data. Around 50% of corotating streams contain energetic ion increases. These increases extend to ~25 MeV/amu, where they merge into the galactic cosmic ray background, and are most evident approaching solar minimum. Sunward ion streaming in the solar wind frame (first-order anisotropy ~20%) and positive radial intensity gradients (~400%/AU) are consistent with acceleration in the outer heliosphere at corotating shocks followed by streaming into the inner heliosphere. The spectra and intensities show little solar cycle variation. The spectra of ions from protons to Fe at ~2–20 MeV/amu are approximated equally well by exponentials in momentum $dJ/dP \approx \exp(-P/P_0)$, P_0 = 11–16 MeV c^{-1} amu^{-1}, or by distribution functions $f \approx \exp(-v/v_0)$, v_0 = 0.18–0.25 (MeV/amu)$^{1/2}$, with equivalent power law in energy slopes in the range ~ −3 to −4. Ion abundances are correlated with the stream peak solar wind speed. In slower corotating streams (maximum solar wind speed <600 km/s), mean abundance ratios are protons/^{4}He = 43 ± 18; ^{4}He/O = 54 ± 23; C/O = 0.62 ± 0.06; Mg/O = 0.19 ± 0.03, and Fe/O = 0.14 ± 0.02. These show some similarity to the corresponding ratios for "solar energetic particles" (SEP) (protons/^{4}He = 70 ± 10; ^{4}He/O = 55 ± 3; C/O = 0.48 ± 0.02; Mg/O = 0.21 ± 0.01 and Fe/O = 0.16 ± 0.02) which are typically accelerated by shocks passing through slow solar wind. In corotating events in higher-speed streams, these ratios become protons/^{4}He = 19 ± 5; ^{4}He/O = 130 ± 35; C/O = 0.89 ± 0.05; Mg/O = 0.14 ± 0.01, and Fe/O = 0.10 ± 0.01 and more closely resemble the corotating event abundance ratios measured in high-speed streams during the mid-1970s solar minimum (protons/^{4}He = 17 ± 7; ^{4}He/O ~ 160 ± 50; C/O = 0.89 ± 0.1; Mg/O = 0.13 ± 0.03, and Fe/O = 0.096 ± 0.05). Solar wind plasma may also show similar variations in composition with solar wind speed (based on the limited solar wind composition measurements available) so that the energetic ion compositions are consistent with the acceleration of corotating event ions and SEPs from the solar wind. The ordering of corotating event and solar wind abundances by first ionization potential and their variation with solar wind speed suggest that conditions in the ion-neutral fractionation region in the upper chromosphere determine the abundances and are associated in some way with regulation of the solar wind speed.

1. INTRODUCTION

Enhancements of MeV/amu ions recurring at the solar rotation period were first identified in 1963 [*Bryant et al.*, 1965] and interpreted as the continuous emission of energetic particles from localized solar regions. Later, *McDonald and Desai* [1971] (see also *Wilcox and Ness* [1965]) noted their association with high-speed solar wind streams corotating with the Sun [*Neugebauer and Snyder*, 1966]. They suggested that the ions escaped along open magnetic field lines above high-speed stream source regions, then termed "M regions", which are now identified with near-equatorial coronal holes [*Hundhausen*, 1979, and references therein].

During the mid-1970s solar minimum, simultaneous observations at 0.3–10 AU from the Sun revealed that corotating events are most intense in the outer heliosphere [*McDonald et al.*, 1976; *Kunow et al.*, 1977; *Van Hollebeke et al.*, 1978; *Christon and Simpson*, 1979] and show sunward streaming in the solar wind frame at 1 AU [*Marshall and Stone*, 1978; *Mewaldt et al.*, 1978; *Christon*, 1981, 1982; *Zwickl and Roelof*, 1981], suggesting that the ions are accelerated in the outer heliosphere rather than at the Sun. In the outer heliosphere, these events are associated with regions of compressed plasma ("corotating interaction regions" (CIRs) [*Smith and Wolfe*, 1977]) formed at the leading edges of corotating high-speed streams by their interaction with the adjacent slower solar wind. Figure 1 shows two corotating solar wind streams and the associated CIRs [after *Belcher and Davis*, 1971]. The dashed arc is the path of a spacecraft at 1 AU relative to the corotating structures. CIRs expand into the slow and fast solar wind, forming shocks if the expansion speed exceeds the magnetosonic speed. This usually occurs in the outer heliosphere where a CIR is typically bounded by a forward shock propagating outward from the Sun and a reverse shock propagating sunward. The energetic ions are found in the vicinity of these shocks, which apparently accelerate the ions [*Barnes and Simpson*, 1976; *Palmer and Gosling*, 1978; *Pesses et al.*, 1978, 1979; *Fisk and Lee*, 1980; *Scholer et al.*, 1980; *Decker et al.*, 1981]. The reverse shock enhancement is generally more intense and has a harder spectrum and a higher He/proton ratio than that at the forward shock [*Barnes and Simpson*, 1976].

Recurrent enhancements in the inner heliosphere may then be due to these ions streaming sunward along magnetic field lines (dotted lines in Figure 1) in the solar wind frame. In particular, ions in high-speed streams at 1 AU are expected to be accelerated at corotating reverse shocks. Since radial intensity gradients are similar for different ions and spectra are independent of heliocentric distance (indicating that propagation is rigidity-independent) [*van Hollebeke et al.*, 1979; *Christon*, 1981; *Richardson*, 1985*a*; see also *Gloeckler et al.*, 1979*b*; *Fisk and Lee*, 1980], corotating event abundances and spectra are expected to be preserved as they propagate toward the Sun. Thus observations at 1

[1]Also at Astronomy Department, University of Maryland, College Park.

Paper number 92JA01837.
0148-0227/93/92JA-01837$05.00

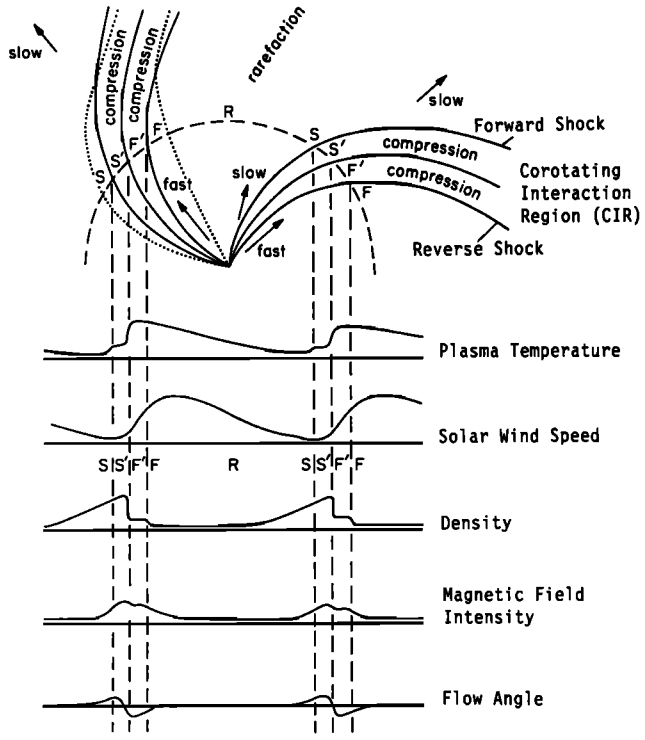

Fig. 1. Schematic of two high-speed streams corotating with the Sun showing typical changes in solar wind parameters at 1 AU [after *Belcher and Davis*, 1971]. S, ambient slow solar wind; S′, compressed, accelerated slow solar wind; F′, compressed, decelerated fast solar wind; F, unperturbed fast solar wind. The S′ and F′ regions, separated by the stream interface, form the corotating interaction region (CIR) which is bounded by forward and reverse shocks in the outer heliosphere. Magnetic field lines (dotted lines) in the S and F regions at 1 AU link to the forward and reverse shocks, respectively.

AU may be used to investigate these events in addition to in situ observations in the outer heliosphere.

Here we discuss the properties of MeV/amu ions at and inside 1 AU associated with corotating high-speed streams from 1978 to 1986 during pre–solar maximum to near solar minimum conditions. Corotating events in this interval have been examined by *Hamilton et al.* [1979], *Decker et al.* [1981], *Richardson and Hynds* [1981, 1990], *Richardson* [1983, 1985*a*, *b*], *Richardson and Zwickl* [1984], *von Rosenvinge and McGuire* [1985], and *Logachev et al.* [1990]. However, these studies only considered a few events from limited time intervals. Here we study 64 corotating solar wind streams using data from the Goddard Space Flight Center (GSFC) energetic particle experiments on the ISEE 3/ICE, Helios 1, and IMP 8 spacecraft.

The spacecraft instruments are described in section 2, while section 3 discusses the event selection. An example of a corotating event is discussed in section 4. Section 5 illustrates the corotation of ion enhancements from Earth to ISEE 3/ICE in 1984–1985. The general properties of corotating events in 1978–1986, including the anisotropy, spectra, and composition, are discussed in section 6, while section 7 summarizes the observations.

2. Instrumentation

The GSFC Medium Energy Cosmic Ray Experiment on ISEE 3/ICE [*von Rosenvinge et al.*, 1978] measures the spectrum, composition, and anisotropy of ≥1 MeV/amu ions. Following launch on August 12, 1978, ISEE 3/ICE orbited the Sun-Earth L1 libration point, 1.5×10^6 km upstream of Earth, from November 1978 until September 1982. From October 1982 until December 1983, the spacecraft was largely in the geomagnetic tail but made occasional excursions into the solar wind. After December 1983, it was placed in a ~1 AU heliocentric orbit and advanced ahead of Earth by ~10° heliolongitude per year, encountering comet Giacobini-Zinner in September 1985 [*von Rosenvinge et al.*, 1986]. The ISEE 3/ICE observations form the foundation of this study, being virtually free of any influence of Earth's bow shock. Thus the duration of this study is limited by the much reduced ISEE 3/ICE data coverage after 1986. The GSFC instrument [*McGuire et al.*, 1986] on IMP 8 (placed in a 40 R_E geocentric orbit) detects >0.5 MeV ions and was operational throughout the study period. Helios 1 was launched in December 1974 into a heliocentric orbit 0.3–1.0 AU from the Sun. Data from the GSFC Helios 1 instrument [*Stilwell et al.*, 1975] are available up to February 1984, though coverage was poor after 1981. Near-Earth solar wind data are obtained from the NSSDC "OMNI" data base [*Couzens and King*, 1986].

3. Selection of Events

To select intervals for study, corotating high-speed solar wind streams (as distinct from high-speed streams associated with travelling interplanetary shocks) were first identified as follows. Figure 1 shows their typical plasma signatures at 1 AU (see also *Belcher and Davis* [1971] and *Hundhausen* [1972]). The solar wind speed rises for ~1 day, followed by a longer decay. The ambient, unperturbed, slow solar wind (S), compressed, accelerated slow solar wind (S′), compressed, decelerated fast solar wind (F′), and unperturbed fast solar wind (F) may be identified. High plasma densities and magnetic field intensities near the leading edge of the high-speed stream (S′ and F′ regions) indicate the CIR. The "stream interface" [*Burlaga*, 1974; *Smith and Wolfe*, 1977] at the S′-F′ region boundary separates slow and fast stream plasma in the centre of the CIR. The stream magnetic field polarity reflects that of the source coronal hole. The streams generally recur at the solar rotation period unless the coronal hole configuration develops from one solar rotation to the next. Recurrent geomagnetic (C9) activity, indicating the passage of corotating streams [*Snyder and Neugebauer*, 1966; *Hundhausen*, 1979], and He 10830 Å coronal hole observations (Solar Geophysical Data) have also been considered in identifying these streams. Also a few streams have been identified from the corotation delay between widely separated spacecraft.

We then examined ISEE 3/ICE energetic particle data and excluded streams containing ions associated with solar particle events and travelling interplanetary shocks (based on the occurrence of prompt high-energy (tens of MeV/amu) ion and energetic electron onsets, strong antisolar streaming during ion onsets and intensity-time profiles, including intensity maxima in the vicinity of travelling shocks. The 64 streams finally chosen are listed in Table 1. The start time is the stream interface passage at ISEE 3/ICE. The finish time corresponds to the trailing edge of the stream except where a field polarity change or a density enhancement, indicating departure from the stream plasma, or a solar particle event

TABLE 1. Corotating High-Speed Streams at ISEE 3/ICE

Interval Date; Hour			1–4 MeV Proton Intensity, $(MeV\ s\ cm^2\ sr)^{-1}$	4–6 MeV/amu, H/He	1.9–2.8 MeV/amu		
Start	End	V_{sw}, km/s			$^4He/O$	C/O	Fe/O
1978							
Nov. 25: 20	Nov. 30; 00	620 ± 10	0.003	6.3 ± 2.0	...	...	...
Dec. 18; 02	Dec. 21; 12	660 ± 10	1	74 ± 12	89 ± 23	0.41 ± 0.20	0.13 ± 0.09
Dec. 22; 08	Dec. 25; 00	550 ± 10	0.05	58 ± 29	...	...	...
Dec. 28; 02	Jan. 2; 00	690 ± 50	3	76 ± 9	106 ± 21	0.83 ± 0.25	...
1979							
April 21; 18	April 23; 00	530 ± 10	0.01	...	...	...	...
May 22: 20	May 26; 00	630 ± 20	0.004	13 ± 9	...	...	...
June 22; 21	June 25; 06	480 ± 20	0.7	39 ± 10	51 ± 24	...	0.33 ± 0.27
July 29; 12	July 31; 08	460 ± 10	0.3	...	...	...	...
Dec. 8; 03	Dec. 12; 00	460 ± 10	0.008	...	...	...	...
1980							
Feb. 26; 02	March 1; 00	560 ± 20	0.08	208 ± 79	...	...	...
Oct. 4; 18	Oct. 5; 18	530 ± 20	2	100 ± 15	70 ± 24	0.36 ± 0.24	...
1981							
Jan. 10; 20	Jan. 14; 00	540 ± 20	0.001	...	...	...	...
June 26; 00	June 28; 00	540 ± 10	8	95 ± 10	43 ± 6	0.60 ± 0.14	0.08 ± 0.04
July 11; 11	July 16; 00	480 ± 10	5	416 ± 93	53 ± 10	0.49 ± 0.16	...
Aug. 27; 20	Aug. 29; 04	540 ± 10	3	280 ± 50	50 ± 11	0,23 ± 0.11	0.33 ± 0.14
Sept. 29; 18	Oct. 1; 12	480 ± 10	3	74 ± 11	58 ± 21	...	...
Dec. 18; 00	Dec. 22; 00	380 ± 10	0.05	80 ± 31	...	...	...
Dec. 24; 00	Dec. 27; 00	470 ± 10	0.1	...	...	...	...
1982							
March 24; 12	March 28; 00	640 ± 10	0.1	...	...	...	...
April 29; 18	May 1; 00	610 ± 10	0.2	...	...	...	...
May 3; 04	May 7; 00	670 ± 20	1	32 ± 2	127 ± 13	0.84 ± 0.13	0.09 ± 0.03
May 26; 12	June 5; 00	750 ± 20	5	22 ± 1	145 ± 8	0.90 ± 0.07	...
July 6; 18	July 9; 00	550 ± 20	0.2	21 ± 1	175 ± 67	1.4 ± 0.7	...
Aug. 2; 12	Aug. 5; 00	600 ± 20	0.6	19 ± 2	178 ± 68	0.77 ± 0.45	...
Aug. 29; 00	Sept. 1; 12	560 ± 20	0.07	17 ± 2	171 ± 100	...	...
Oct. 10; 15	Oct. 15; 00	510 ± 20	0.4	28 ± 3	97 ± 57	...	...
1983							
Sept. 8; 18	Sept. 14; 12	560 ± 10	0.01	7 ± 2	...	...	...
Sept. 25; 00	Sept. 27; 12	690 ± 10	1.5	33 ± 5	130 ± 30	1.08 ± 0.35	...
Oct. 6:14	Oct. 10; 12	570 ± 10	0.04	10 ± 2	52 ± 31	...	2.3 ± 1.6
Oct. 28; 22	Oct. 31; 12	530 ± 10	0.02	30 ± 8	59 ± 43	1.6 ± 1.5	...
Nov. 2; 04	Nov. 7; 00	660 ± 20	2	130 ± 19	58 ± 14	0.23 ± 0.13	...
Nov. 15; 15	Nov. 23; 00	850 ± 50	0.2	53 ± 19	...	...	...
Nov. 24; 18	Nov. 27; 00	470 ± 20	0.01	...	...	...	...
Dec. 5; 18	Dec. 9; 00	630 ± 20	0.03	...	...	...	...
Dec. 12; 00	Dec. 15; 00	700 ± 10	1	26 ± 3	115 ± 27	1.0 ± 0.3	0.11 ± 0.08
1984							
Jan. 28; 03	Jan. 30; 04	550 ± 20	0.07	3.8 ± 1.4	...	...	...
March 28; 12	April 1; 00	750 ± 10	0.009	...	...	...	...
June 16; 11	June 18; 00	700 ± 30	1.3	116 ± 67	74 ± 53	...	...
July 17; 12	July 24; 00	600 ± 50	2.02	20 ± 1	115 ± 20	0.36 ± 0.13	0.15 ± 0.07
Aug. 3; 12	Aug. 9; 00	660 ± 30	0.081	51 ± 16	...	...	...
Aug. 16; 00	Aug. 20; 00	610 ± 20	0.2	17 ± 5	...	...	...
Aug. 29; 00	Sept. 2; 00	640 ± 30	3	14 ± 1	132 ± 19	0.54 ± 0.13	0.18 ± 0.07
Sept. 11; 00	Sept. 21; 00	790 ± 20	0.7	43 ± 6	241 ± 73	1.0 ± 0.4	...
Sept. 24; 12	Oct. 2; 00	770 ± 20	3	29 ± 5	157 ± 53	1.3 ± 0.6	...
Oct. 8; 00	Oct. 18; 00	795 ± 100	4	14 ± 1	183 ± 24	1.14 ± 0.21	0.17 ± 0.06
Oct. 20; 00	Oct. 25; 00	800 ± 50	1	26 ± 5	170 ± 86	1.6 ± 1.1	...
Nov. 2; 12	Nov. 10; 00	700 ± 50	7	13 ± 1	134 ± 18	0.88 ± 0.15	0.06 ± 0.03
Nov. 16; 12	Nov. 24; 00	650 ± 50	0.3	26 ± 5	105 ± 40	0.6 ± 0.4	...
Nov. 30; 00	Dec. 11; 00	850 ± 100	30	30 ± 2	194 ± 18	0.99 ± 0.13	0.04 ± 0.02
Dec. 28; 00	Jan. 7; 00	800 ± 50	0.3	28 ± 3	204 ± 78	1.1 ± 0.6	...
1985							
Jan. 9; 18	Jan. 16; 00	700 ± 50	1	26 ± 9	205 ± 104	...	...
Feb. 6; 00	Feb. 9; 00	790 ± 50	0.2	...	...	...	...
March 6; 00	March 12; 00	810 ± 50	0.2	...	...	...	...
April 2; 00	April 6; 00	740 ± 20	...	...	...	...	...
July 25; 00	July 29; 00	570 ± 30	0.05	71 ± 41	...	...	...
Aug. 15; 00	Aug. 20; 00	640 ± 20	0.02	...	...	...	...
Oct. 7; 12	Oct. 13; 00	700 ± 20	0.1	5.3 ± 3.3	...	...	...
Nov. 4; 12	Nov. 10; 00	650 ± 50	0.04	...	...	...	...
Nov. 15; 00	Nov. 18; 00	700 ± 20	0.01	...	...	...	...
Nov. 30; 00	Dec. 6; 00	600 ± 50	1	20 ± 10	...	...	...
Dec. 12; 12	Dec. 17; 00	750 ± 50	0.01	...	...	...	...
Dec. 30; 00	Jan. 4; 00	750 ± 20	0.6	...	...	...	...
1986							
June 3; 12	June 12; 00	530 ± 20	1.5	25 ± 4	180 ± 49	0.85 ± 0.34	...
June 30; 12	July 7; 00	570 ± 20	0.2	...	...	...	...

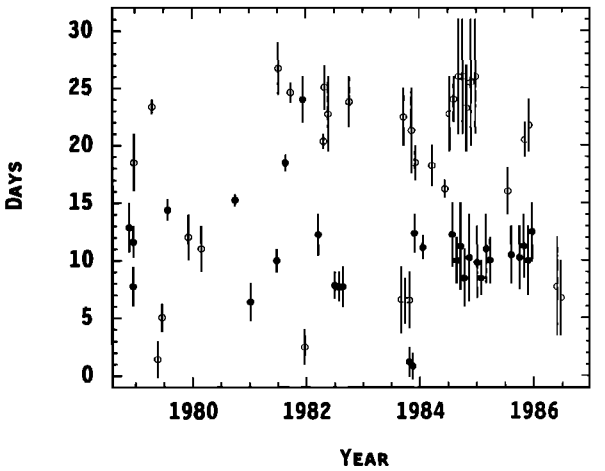

Fig. 2. The corotating streams in Table 1 plotted in a 27-day solar rotation interval format with a 1- and 5-day overlap at the start and end of each interval. Streams marked with solid (open) circles contain outward (sunward) directed magnetic field.

onset, occurred earlier. The 1978–1982 streams show excellent agreement with the corotating streams identified independently by *Lindblad et al.* [1989]. Those in 1978–1981 show no association with the intervals of solar flare dominated ion fluxes identified by *Shields et al.* [1985]. The intervals are plotted in Figure 2 in a 27-day solar rotation format (with an overlap of 1 and 5 days at the beginning and end of each 27-day period) in which corotating structures form a horizontal sequence. Solid and open circles denote streams with outward (positive) or sunward (negative) interplanetary magnetic field (IMF), respectively. Corotating streams were present at all levels of solar activity, with clear recurrence in 1983–1986 approaching solar minimum (see also *Logechev et al.* [1990]).

Table 1 also shows the peak solar wind speed in each stream (obtained from 1-hour-averaged OMNI data) together with the peak 1–4 MeV proton intensity and various ion abundance ratios derived from ISEE 3/ICE data, to be discussed below. Figure 3 shows pulse-height matrices illustrating the response of the ISEE-3/ICE very low energy telescope (VLET) D1 and D2 detectors to heavy ions during these events and large solar energetic particles (SEP) events. The left-hand panel shows the distribution for a sample of large SEP events during the first half of 1981, included in the analysis of such events by *Cane et al.* [1991]. The various elemental tracks can be easily distinguished. The right-hand panel shows the combined distribution for the corotating streams in Table 1. The elemental tracks are again evident, though less clearly due to the fewer particle counts associ-

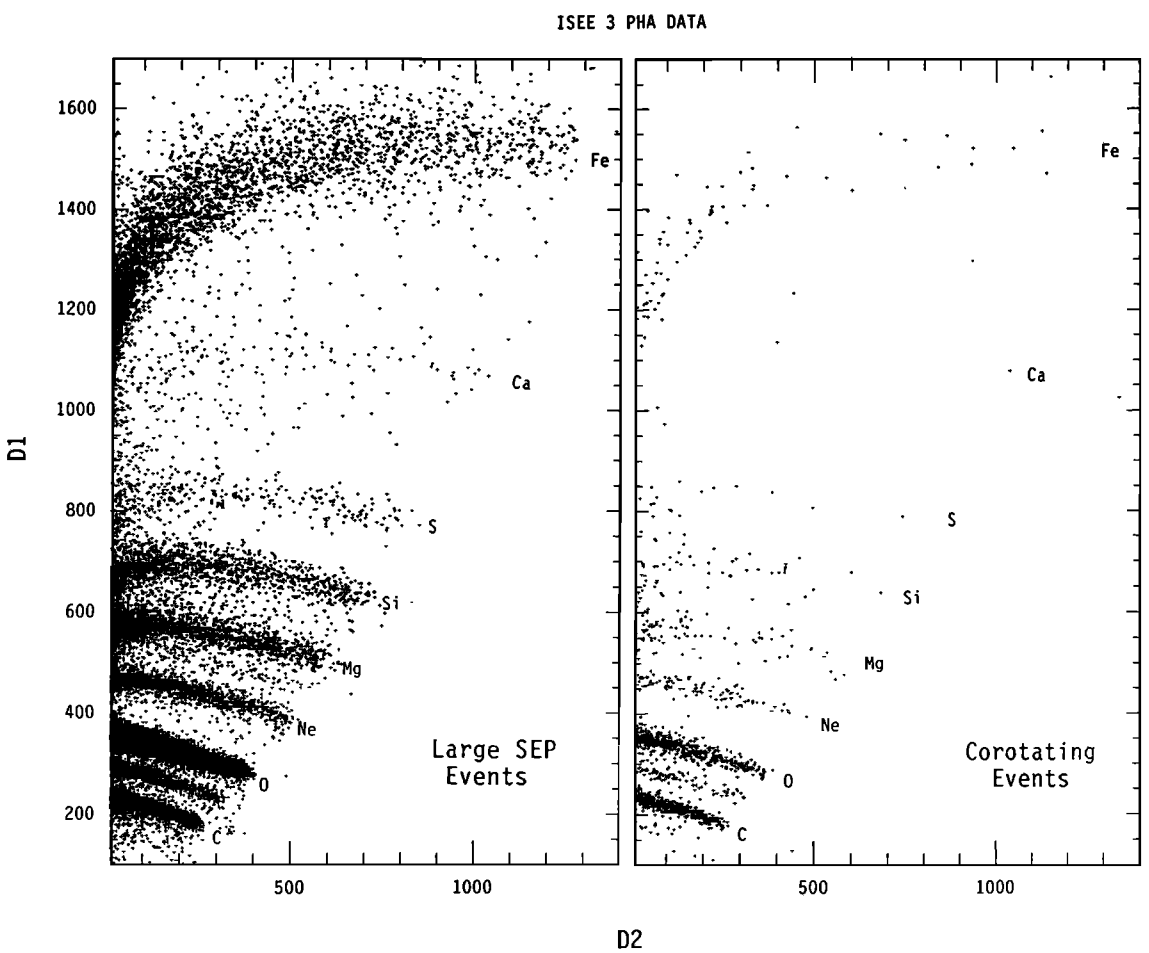

Fig. 3. ISEE 3/ICE VLET D1 and D2 detector pulse-height matrices for a sample of large SEP events during the first half of 1981 (left-hand panel) and summed over the corotating stream intervals in Table 1 (right-hand panel), showing the response to ions of varying type.

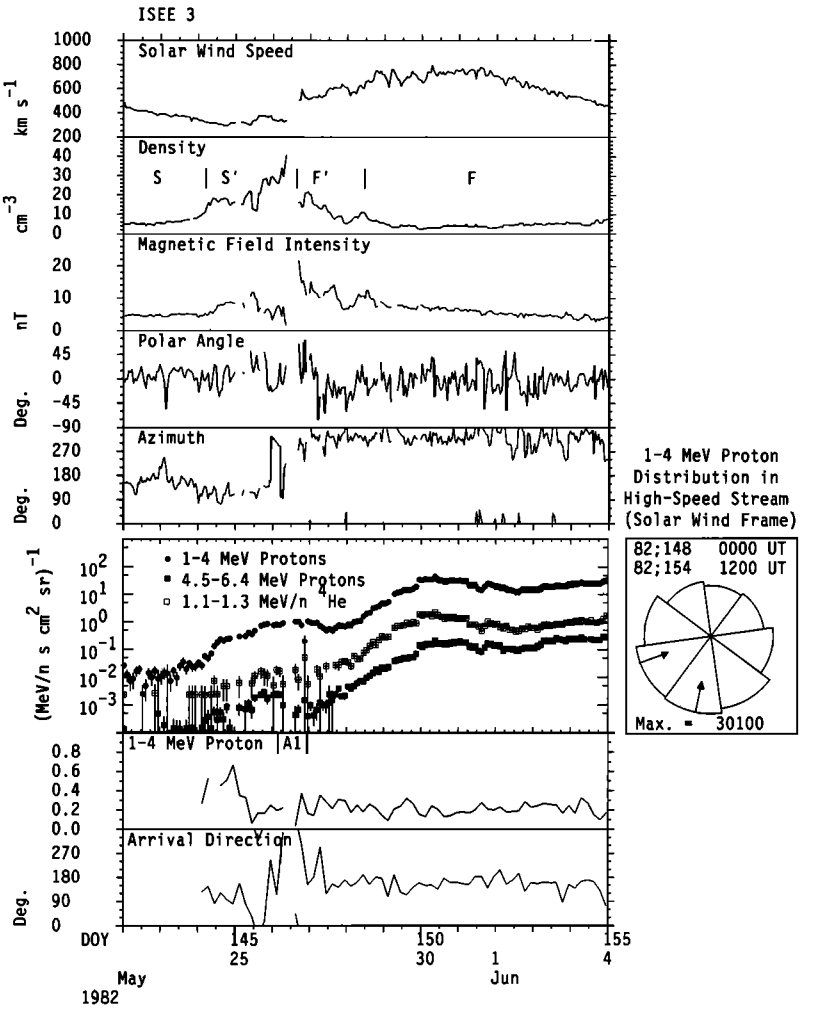

Fig. 4. ISEE 3/ICE solar wind and energetic ion observations for May 22 to June 3, 1982, showing an energetic ion enhancement associated with a corotating high-speed stream. The pie plot shows the solar wind frame 1–4 MeV proton azimuthal intensity during the enhancement, plotted versus viewing direction with the Sun to the top of the figure. The mean magnetic field azimuth and the number of counts in the maximum flux sector are indicated.

ated with the corotating streams. In particular, only a few Ca and S counts are apparent.

4. An Example of a Corotating Particle Event

Figure 4 shows solar wind and energetic ion data associated with a corotating high-speed stream which passed the Earth on May 26 to June 4, 1982, and originated in an equatorward extension of the northern polar coronal hole (Solar Geophysical Data, *456*, Part 1, p. 52). The unperturbed slow (S) and fast solar wind (F) are separated by a CIR including a stream interface which apparently passed by during the data gap at ~1200 UT on May 26. Forward and reverse shocks may form at the edges of the CIR (S-S' and F'-F region boundaries, respectively) in the outer heliosphere. A solar particle event commenced late on June 3, so later observations are not shown.

The 2-orders-of-magnitude MeV/amu ion increase in the high-speed stream following CIR passage occurs on field lines which are expected to connect to the CIR reverse shock in the outer heliosphere (see Figure 1). The pie plot shows the 1–4 MeV proton azimuthal intensity distribution during this increase transformed into the solar wind frame using the method of [*Gold et al.*, 1975]. Fluxes in eight azimuthal sectors about the spacecraft are plotted versus viewing direction with the Sun to the top of the figure. Arrows indicate ±1 standard deviation from the mean magnetic field direction. The maximum sector ion count is also given. The sunward, field-aligned streaming in the solar wind frame is consistent with a positive radial ion intensity gradient resulting from ion acceleration in the outer heliosphere. The bottom two plots in Figure 4 show the first harmonic magnitudes A_1 and arrival directions (0° is antisolar radial flow) obtained from Fourier fits [*Zwickl and Webber*, 1976] to 4-hour-averaged sectored data. In the high-speed stream, $A_1 \sim 20\%$, directed sunward along the spiral magnetic field direction ($\Phi \sim 150°$ for a ~700 km/s solar wind speed).

In addition, a "precursor" ion increase commences at the CIR leading edge. The predominantly sunward flow indicates an outer heliosphere source. However, field lines within the CIR at 1 AU are not expected to connect with the outer heliosphere corotating shocks (Figure 1). These ions may have diffused across field lines in the outer heliosphere from the corotating shocks or may be stochastically accel-

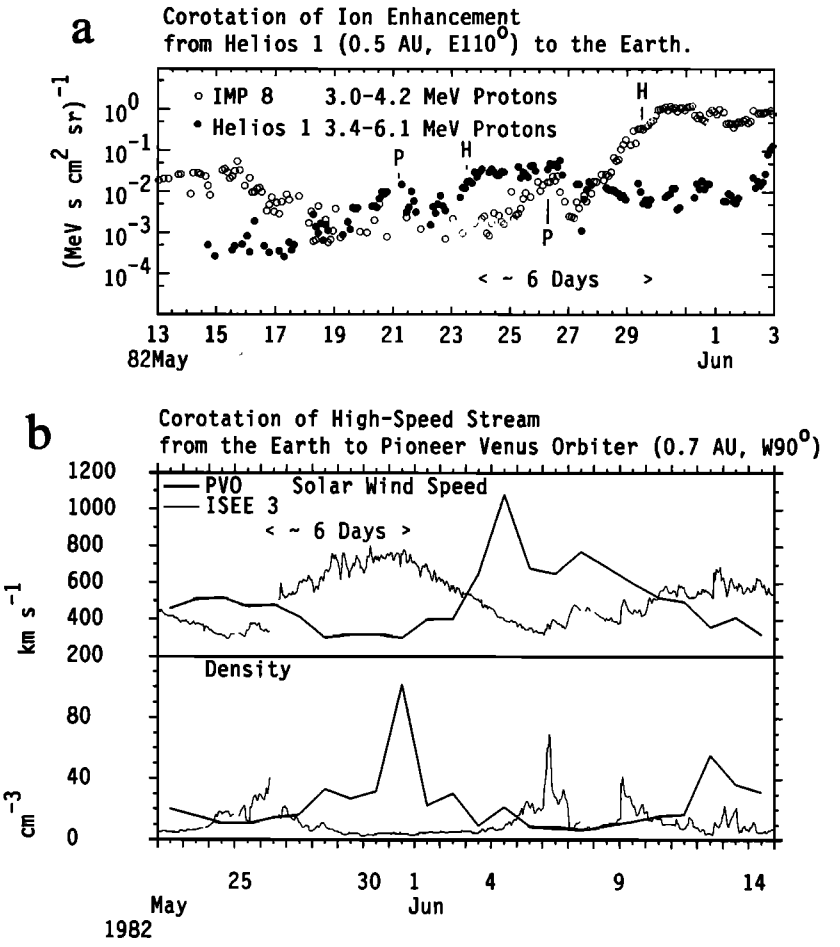

Fig. 5. (*a*) ~3 MeV proton data from Helios 1 and IMP 8 showing that the high-speed stream-associated ion enhancement in Figure 4 (H) corotated past Helios 1 (at 0.5 AU, 110° east of Earth) ~6 days before it was observed at Earth and was around an order of magnitude less intense at Helios 1. The precursor enhancement (P) shows little change in intensity. (*b*) The high-speed stream and CIR in Figure 4 corotated past Pioneer Venus Orbiter at 0.7 AU, ~90° west of Earth around 6 days after passing Earth.

erated within the CIR in the outer heliosphere by turbulence generated by the stream interaction [*McDonald et al.*, 1976]. No sunward streaming ion increase is observed in the slow solar wind (S region) on field lines which are expected to connect with the CIR forward shock in the outer heliosphere (Figure 1).

Figure 5*a* shows that the high-speed stream-associated ion event (H) and its precursor (P) were observed by IMP 8 at Earth ~6 days after passing Helios 1 at 0.5 AU, 110° east of Earth, consistent with the expected corotation delay of ~7 days. The 3.0–4.2 MeV ion intensity at IMP 8 was around an order of magnitude greater than at Helios 1 in a similar (but not identical) energy range (3.4–6.1 MeV). This indicates that the ion intensity increased with heliocentric distance, assuming that little event development occurred as the event corotated between Helios 1 and Earth. To estimate the radial gradient, we have compared the 3.4–6.1 MeV proton intensity from Helios 1 with the sum of the 3.0–4.2 MeV proton intensity from IMP 8 and the 4.5–6.4 MeV proton intensity from ISEE 3 (not shown in Figure 5) in order to estimate the 1-AU intensity over a similar energy range. This gives a gradient of ~520%/AU which is reduced to ~400%/AU if a correction is made for the remaining difference in energy ranges, assuming a typical power law spectral index of −3.5 (as obtained in section 6.3). This gradient is similar to the ~350%/AU gradients observed in the inner heliosphere during mid-1970s solar minimum corotating events [*van Hollebeke et al.*, 1978; *Kunow et al.*, 1977]. On the basis of a steady state diffusion-convection propagation model, the gradient (G) and solar wind frame (diffusive) anisotropy (event-averaged mean $A_1 = 21 \pm 1\%$) may be related by a field-aligned mean free path $\lambda_\parallel = A_1/(G \cos^2 \Phi)$ [*Fisk*, 1976], where Φ is the angle between the radial and magnetic field directions (~30° at 1 AU for 700 km/s solar wind). If $G \approx 400\%/AU$, then $\lambda_\parallel \approx 0.06$ AU, consistent with previous estimates of 0.03–0.11 AU obtained by *Kunow et al.* [1977], *Mewaldt et al.* [1978], and *Christon* [1981] from corotating events. The precursor event shows little intensity difference between Helios 1 and Earth, even though the sunward streaming suggests that a positive radial gradient existed. It is possible that the precursor developed while corotating from Helios 1 to Earth, resulting in a fall in the intensity in the inner heliosphere and thereby setting up the positive radial gradient.

Figure 5*b* shows that the high-speed stream and CIR density enhancement were observed at Pioneer Venus Orbiter (located at 0.7 AU, 90° west of Earth; data from Solar

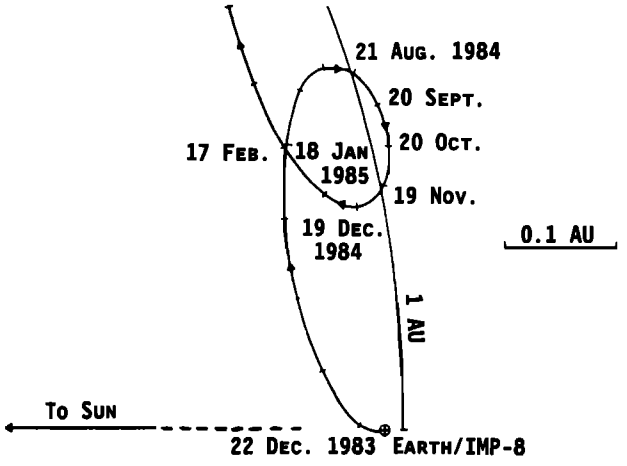

Fig. 6. ISEE 3/ICE heliocentric trajectory relative to a fixed Sun–Earth line from December 1983 to early 1985 [after *von Rosenvinge et al.*, 1986].

Geophysical Data) some 6 days after passing Earth, again consistent with corotation.

5. Corotation of Events From Earth to ISEE 3 in 1984–1985

In December 1983, ISEE 3/ICE was placed in a ~1-AU heliocentric orbit in which it advanced ahead of Earth by ~10°/yr (Figure 6). Thus the prominent recurrent events in Figure 2 between mid-1984 and early 1985 [*Logachev et al.*, 1990; *von Rosenvinge and McGuire*, 1985] would be expected to be observed with a corotation delay of ~1 day between Earth and ISEE 3/ICE.

Figure 7 shows IMP 8 and ISEE 3/ICE ~1 MeV proton intensities, daily geomagnetic C9 indices (Solar Geophysical Data) and IMF polarities at Earth (where positive (negative) indicates antisolar (sunward) directed field) for five solar (Bartels) rotations in September 1984 to January 1985. Two intervals of recurrent geomagnetic activity occur each solar rotation, each contained within one magnetic sector. The near-Earth solar wind data are incomplete and so are not plotted here. Instead, thick horizontal bars indicate when the two corotating streams responsible for the geomagnetic activity passed ISEE 3/ICE [*von Rosenvinge and McGuire*, 1985].

The proton data are dominated by two recurrent particle enhancements during each solar rotation. These were observed at ISEE 3/ICE a day or so later than at Earth, consistent with corotation. The ion events are clearly long-lived spatial structures rather than temporal features and are associated with the recurrent geomagnetic activity and corotating high-speed streams. The 1–4 MeV/amu ion angular distributions at ISEE 3/ICE during each recurrent event (transformed into the solar wind frame using ISEE 3/ICE solar wind data from *von Rosenvinge and McGuire* [1985] and showing some broadening due to field direction changes during the integration periods) are shown in Figure 7. The sunward field-aligned streaming is consistent with an outer heliosphere source. These are among the most intense corotating events identified during the study interval (as will be seen from Figure 9 below). In contrast, no ion enhancements precede the geomagnetic activity intervals and high-speed streams, suggesting that ions from corotating forward shocks were not observed at 1 AU.

The top panel of Figure 8 shows rotation-to-rotation variations in the proton and ^{4}He intensities during the two corotating streams. The stream magnetic field polarity is indicated. (The positive polarity stream on December 12–22 is omitted because of geomagnetic storm sudden commencements on December 13 and 21 that may be associated with travelling shocks.) In the negative stream (data points joined by solid lines), the ~1 MeV/amu ion intensity increases for four rotations and then decreases on the fifth. The positive stream intensity (dashed lines) is generally lower and falls slightly over the first three rotations followed by a slight rise on the last rotation plotted. Thus there is no systematic intensity variation from one solar rotation to the next in these events.

The second and third panels show the He/O and C/O abundance ratios at 1.9–2.8 MeV/amu. These may be compared with typical values included in Table 2 for solar energetic particles (SEPs) (from *Cane et al.* [1991], also from the GSFC ISEE 3/ICE instrument) and for corotating event ions at 1 AU (compiled from reports by *Gloeckler et al.* [1979*a*, *b*], *Scholer et al.* [1979], *McGuire et al.* [1978], *Christon and Simpson* [1979], and *von Rosenvinge and McGuire* [1985]), obtained during solar minimum conditions in the mid-1970s (except for *von Rosenvinge and McGuire* [1985]) and henceforth referred to as "solar minimum corotating event" (SMCE) abundances. The abundance ratios vary from rotation to rotation and are generally consistent with SMCE abundances but are occasionally more SEP-like. There is a possible correlation between these ratios and the stream peak solar wind speed, shown in the bottom panel, which will be investigated below for all events in this study. The bottom panel shows spectral indices (μ) obtained from fitting power laws in energy ($dJ/dE \approx E^{-\mu}$) to He, C, and O intensities at 1.9–2.8 and 4–7 MeV/amu. These range from ~2.5 to 5.2 and are generally similar for each ion type. There is no general trend from one rotation to the next.

6. General Characteristics of Corotating Events

6.1. *Intensity and Spatial Structure*

We now consider some general features of corotating events in 1978–1986. The top panel of Figure 9 illustrates that the peak 1–4 MeV proton intensity shows little variation between solar maximum conditions in 1979–1981 and solar minimum conditions in the mid-1980s, suggesting that ambient low-energy solar particles, which are expected to be more abundant around solar maximum, do not provide a significant "seed" population for acceleration by corotating shocks. The ion intensity may be expected to be related to the shock strength which may be correlated to the high-speed stream speed or to the difference between slow- and high-speed solar wind speeds. The bottom panels in Figure 9 show peak 1–4 MeV proton and mean 7–13 MeV proton and 1.10–1.34 MeV/amu ^{4}He intensities plotted against the maximum solar wind speed in each stream. The symbol size indicates the magnitude of the solar wind speed increase. There is a slight tendency for higher ion fluxes to be associated with faster streams and with greater speed increases, but overall the ion intensity is relatively independent of these parameters.

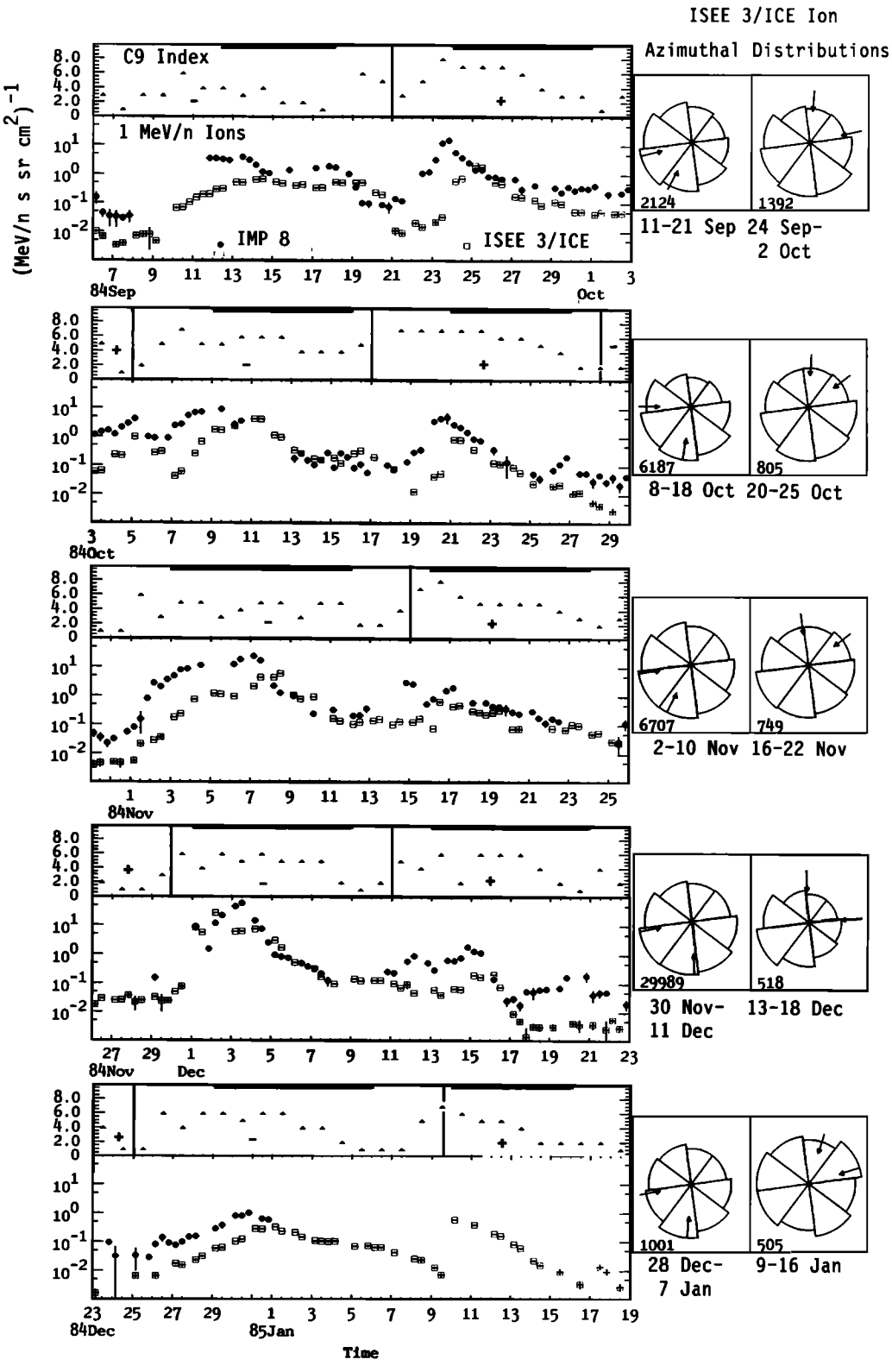

Fig. 7. Two recurrent ~1 MeV ion enhancements, observed over five solar rotations in September 1984 to January 1985, which corotated past ISEE 3/ICE ~1 day after passing IMP 8. The enhancements occurred within sectors of predominantly outward (positive) or sunward (negative) magnetic field and were associated with recurrent enhanced geomagnetic activity (indicated by the C9 index) due to the passage of corotating high-speed streams which passed ISEE 3/ICE at the times indicated by horizontal bars. The azimuthal ion intensity plots for the two enhancements in each solar rotation indicate sunward field-aligned streaming in the solar wind frame.

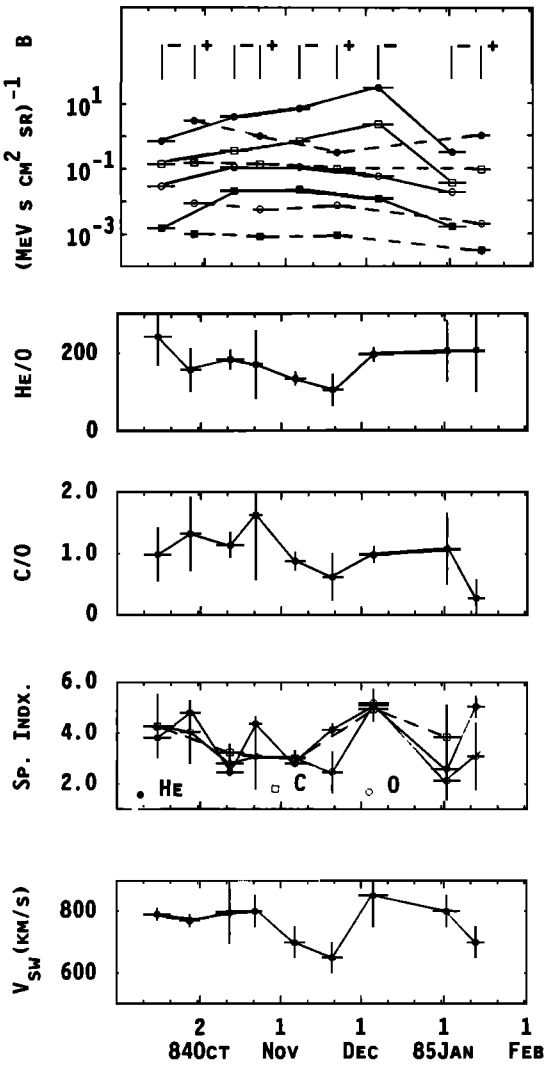

Fig. 8. Variation on successive solar rotations of proton and ^{4}He intensities (solid circles, 1–4 MeV protons; open squares, 1.10–1.34 MeV/amu ^{4}He; open circles, 4.5–6.4 MeV protons; solid squares: 3.7–5.4 MeV/amu ^{4}He), ^{4}He/O and C/O ion abundance ratios, ^{4}He, C, and O spectral indices at 1.9–7 MeV/amu, and the maximum solar wind speed for the two corotating streams in Figure 7. Solid and dashed lines join intensity data points for streams containing sunward (negative) and antisolar (positive) directed magnetic field, respectively.

In several streams, the 1–4 MeV proton intensity approaches "quiet time" levels ($\leq 10^{-2}$ (MeV s cm^2 sr)$^{-1}$ [*Richardson et al.*, 1990]), in contrast to the ion enhancements in Figures 4 and 7. Figure 10 shows an "empty" stream observed on two solar rotations. This closely follows another corotating stream (the CIRs are less than a quarter of a solar rotation apart) and interacts with its trailing edge on the second rotation. Dashed vertical lines indicate the stream interface which ions in the preceding solar wind apparently do not cross. The CIR on November 25–26, 1978, in the top panel was bounded by a corotating forward-reverse shock pair at 1 AU. Ion enhancements extending to a few hundred keV were present at these shocks [*Richardson and Zwickl*, 1984] (though in Figure 10, only the forward shock enhancement is evident at 1–4 MeV) so ion acceleration must have been taking place at 1 AU. However, the absence of ions in the high-speed stream suggests that acceleration at the reverse shock did not extend to much beyond 1 AU. The presence of closely spaced streams here (and in several other cases examined) suggests that empty streams may occur when two corotating streams closely spaced in heliolongitude interact just beyond 1 AU. The resulting CIR is likely to be weaker, due to the smaller difference in solar wind speed, and is presumably less likely to be bounded by developed shocks in the outer heliosphere. Or, if as in the top panel of Figure 10, shocks are formed at 1 AU, they may be weakened as the high-speed streams interact in the outer heliosphere, accounting for the absence of accelerated ions in the stream at 1 AU. The merging of streams and CIRs has been observed in the outer heliosphere (at several AUs) and reviewed by *Whang* [1991]. Here we suggest that merging may occasionally occur rather closer to the Sun between closely spaced streams. We also note that various attempts have been made to relate the November 25, 1978, shock to a solar event [*Joselyn and McIntosh*, 1981; *Sanahuja et al.*, 1983; *Tang et al.*, 1989; *Perez-Enriquez and Mendoza*, 1990], whereas the observations presented here (and by *Richardson and Zwickl* [1984]) suggest that this was a rare (but not unique [*Chao et al.*, 1972; *Dryer*, 1975; *Armstrong et al.*, 1977]) example of a corotating shock at 1 AU.

We estimate that ~20% of the streams in our study show an MeV/amu ion enhancement at 1 AU commencing after passage of the trailing edge of the CIR (i.e., observed only on field lines connecting to the reverse shock). In another ~30%, the ion enhancement commences inside the CIR (as

TABLE 2. Abundances (O ≡ 1) at 1.9–2.8 MeV/amu

		Corotating Events			
	SEP[a]	1978–1981	1982–1983	1984–1986	SMCE[b]
^{4}He	55 ± 3	52 ± 15	123 ± 35	148 ± 33	160 ± 50
C	0.48 ± 0.02	0.50 ± 0.07	0.86 ± 0.06	0.90 ± 0.06	0.89 ± 0.1
N	0.13 ± 0.01	0.093 ± 0.024	0.17 ± 0.02	0.15 ± 0.02	0.14 ± 0.01[c]
Ne	0.15 ± 0.01	0.15 ± 0.03	0.16 ± 0.02	0.19 ± 0.02	0.20 ± 0.04
Mg	0.21 ± 0.01	0.22 ± 0.04	0.15 ± 0.02	0.13 ± 0.02	0.13 ± 0.03
Si	0.15 ± 0.01	0.13 ± 0.03	0.11 ± 0.02	0.08 ± 0.01	0.08 ± 0.02
S	0.035 ± 0.004	0.042 ± 0.016	0.042 ± 0.01	0.06 ± 0.01	0.06 ± 0.01
Fe	0.16 ± 0.02	0.13 ± 0.03	0.12 ± 0.02	0.092 ± 0.015	0.096 ± 0.05

[a]Solar energetic particles, *Cane et al.* [1991].
[b]Solar minimum corotating events: *Gloeckler et al.* [1979*a*, *b*], *Scholer et al.* [1979], *McGuire et al.* [1978], *Christon and Simpson* [1979], and *von Rosenvinge and McGuire*, [1985].
[c]*Reames et al.* [1991].

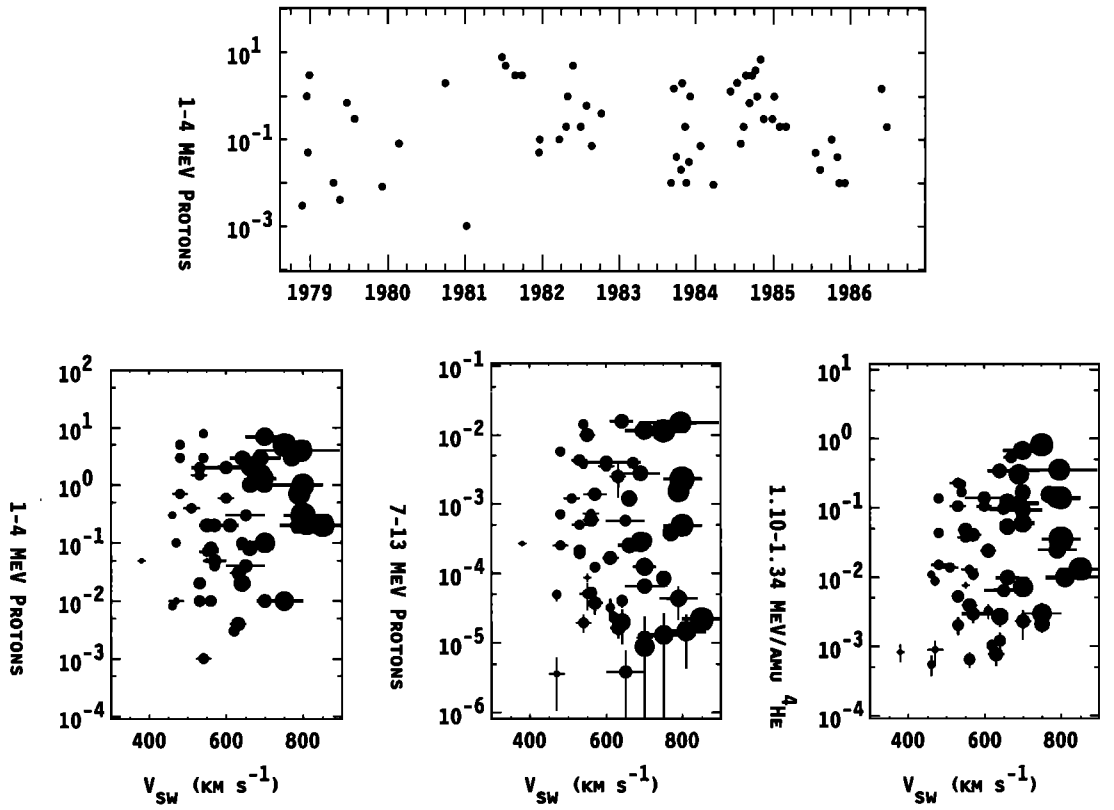

Fig. 9. (Top) 1–4 MeV proton intensity (MeV s cm^2 sr)$^{-1}$ in corotating streams versus date of observation, showing no clear solar cycle dependence. (Bottom) Proton and ^{4}He intensities ((MeV/amu s cm^2 sr)$^{-1}$) versus maximum solar wind speed in each stream. The symbol size indicates the solar wind speed increase from the preceding slow solar wind to the high-speed stream. The ion intensity is relatively independent of these parameters.

in Figure 4) and extends into the high-speed stream (suggesting that energetic ions are frequently observed inside the CIR at 1 AU on field lines which are not expected to link with the corotating shocks.) Thus around 50% of fast streams include significant particle enhancements above ambient flux levels. Some 20% show increases in the preceding slow solar wind which do not extend across the stream interface (as in Figure 10). These may be sunward streaming ions from corotating forward shocks or from the decay phase of solar particle events. Around 15% show no enhancements either in the preceding slow solar wind or within the high-speed stream.

6.2. *Anisotropy*

Figure 11*a* shows the first harmonic $\mathbf{A}_1$ in the spacecraft frame of ISEE 3/ICE 1–4 MeV proton azimuthal directional fluxes summed over each event. The ions arrive predominantly from ~350°–90° (i.e., from the east of the Sun approximately along the corotation **E** × **B** drift direction) with a small first-order anisotropy (~5–30%) (which may be slightly underestimated due to broadening arising from magnetic field direction variations during the long integration periods). The streaming is not in general away from the Sun along the average field direction ($\Phi \approx 315°$–$330°$) and hence is inconsistent with steady particle emission from the Sun. Figure 11*b* shows the first-order anisotropy in the solar wind frame. Here, $A_1 \approx 5$–40%, and $\Phi \approx 110°$–$210°$, centered around ~150°, close to the average sunward field direction ($\Phi \approx 146°$) for ~600 km/s solar wind, indicating weak, field-aligned, sunward streaming consistent with the anisotropies reported by *Marshall and Stone* [1978], *Mewaldt et al.* [1978], *Christon* [1981, 1982], *Zwickl and Roelof* [1981], and *Richardson* [1985*a*].

In section 4, the mean free path was estimated for one stream by combining the anisotropy with a Helios 1 to Earth intensity gradient. It is difficult to identify unambiguously other corotating events at both spacecraft due to the large number of solar particle events around solar maximum, when simultaneous data coverage was greatest, and to the poor Helios coverage after 1981 when corotating streams were more apparent. However, assuming positive radial gradients similar to those previously reported (~350–400%/AU) and a steady state diffusion-convection model, the anisotropies (5–40%) are consistent with mean free paths of the order of ~0.01–0.1 AU.

6.3. *Spectra*

Figure 12 shows ~1–50 MeV/amu ion spectra summed over the events in Table 1 observed between 1982 and 1986 when corotating streams were most prominent. The spectra are plotted such that linear fits are produced by (1) power law in energy spectra ($dJ/dE \approx E^{-\mu}$); (2) exponentials in momentum (P) ($dJ/dP \approx \exp(-P/P_0)$), and (3) exponential in velocity distribution functions ($f \approx \exp(-v/v_0)$), in the left-hand, center, and right-hand panels, respectively. The best fit values of μ, P_0, and v_0 for each ion type in the ranges specified are also indicated. The proton spectrum above ~2 MeV in the left-hand panel is approximated by a power law

in energy (form 1) with $\mu = 4.17 \pm 0.19$, similar to the spectra reported by *Kunow et al.* [1977] ($\mu = 4$ at 4–13 MeV) and *Logachev et al.* [1990] ($\mu = 4.0$–5.0 at >1 MeV in recurrent events in 1985). The spectrum may also be fitted to forms 2 and 3, with $P_0 = 16.5 \pm 0.1$ MeV/c (consistent with work by *van Hollebeke et al.* [1979]) or $v_0 = 0.25 \pm 0.03$ (MeV)$^{1/2}$, respectively. Above ~40 MeV, the spectrum merges into the galactic cosmic ray (GCR) spectrum. Because of the broad channel at the lowest proton energy (1–4 MeV), the proton spectrum below 4 MeV is poorly defined. However, somewhat harder power law and exponential in momentum spectra have been reported by *Marshall and Stone* [1978] ($\mu = 3.0 \pm 0.8$ at 1.3–2.3 MeV) and at ≤1 MeV by *Zel'Dovich et al.* [1981] ($\mu = 1.2$–2.5, $P_0 = 7$–10 MeV/c at 30–750 keV), *Richardson and Hynds* [1990] ($\mu = 1.1$–3.0, $P_0 = 5$–9 MeV/c) at 35–1600 keV), and *Logachev et al.* [1990] ($\mu = 0.3$–3.0 at <1 MeV). Similar spectra with $\mu \approx 2$ are also found for 0.54–1.85 MeV protons at corotating reverse shocks in the outer heliosphere [*Barnes and Simpson*, 1976]. Taken together, the observations indicate that corotating event proton spectra extend down to ≤30 keV,

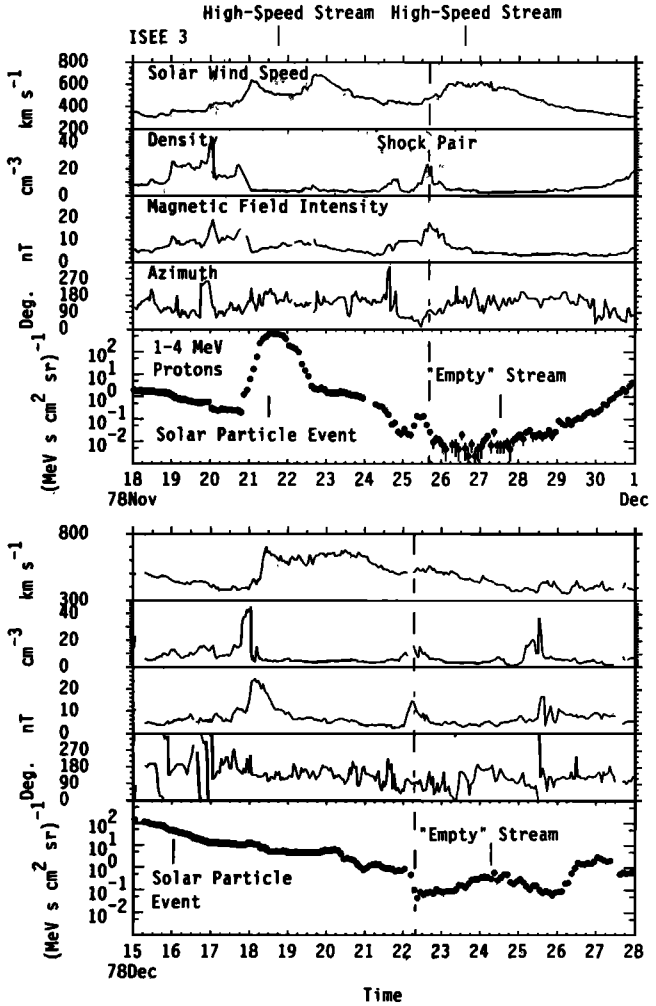

Fig. 10. An "empty" high-speed stream including low particle fluxes observed on two solar rotations. Vertical dashed lines denote the stream interface. This stream closely follows another corotating stream and merges with its trailing edge on the second rotation. The CIR on November 25–26, 1978, was bounded by a corotating forward-reverse shock pair at 1 AU.

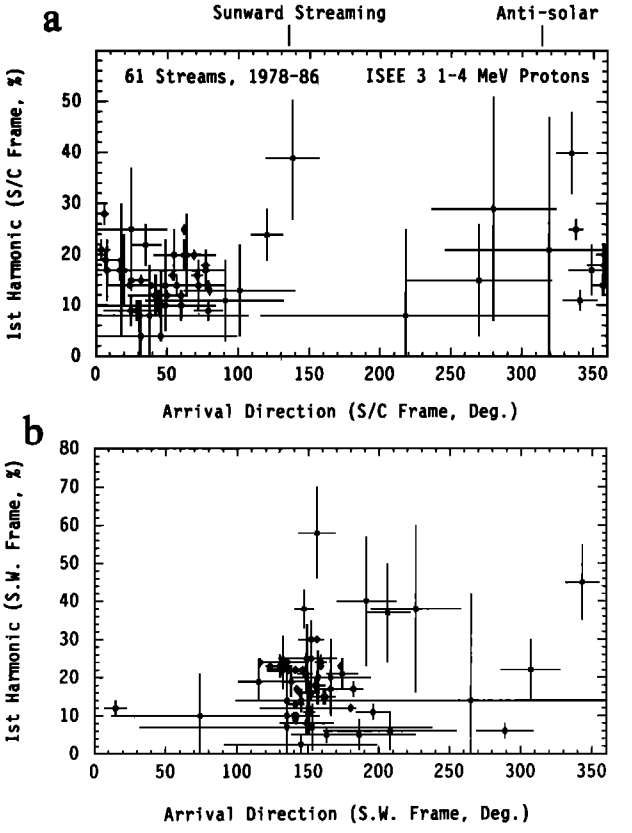

Fig. 11. (*a*) The 1–4 MeV proton streaming (first harmonic, A_1) in the spacecraft frame for the events in Table 1. Particles arrive from ~350°–90° (i.e., approximately along the **E** × **B** drift direction) with a first-order anisotropy ~5–30%. (*b*) The 1–4 MeV proton streaming in the solar wind frame. A weak ($A_1 \approx 5$–40%), predominantly sunward field-aligned (~110°–210°) streaming is found.

with no low-energy turndown (indicating that the seed particle population must lie at lower energies), may harden slightly at <3 MeV and extend up to energies of ~30 MeV where they merge into the GCR background.

The ^{4}He spectrum in Figure 12 has better energy resolution below 4 MeV/amu. Represented as a power law in energy, the spectrum is harder below ~3 MeV/amu than at higher energies, μ increasing from ~2.6 to ~4.1, suggesting (from the discussion in the previous paragraph) that the ^{4}He and proton MeV/amu spectra are of similar forms. Again the spectrum merges with the GCR spectrum above ~20 MeV/amu. The center and right-hand panels show that forms 2 and 3 in fact provide excellent fits to the ^{4}He spectrum. Heavier ion observations are limited to ~2–12 MeV/amu (2–24 MeV/amu for Fe). The spectra are generally consistent with those of protons and ^{4}He in this energy range but are not uniquely fitted by any one spectral form. In particular, the spectral parameters ($\mu = 3.1$–4.3, $P_0 = 10.8$–16.5 (MeV c^{-1} amu^{-1}) and $v_0 = 0.18$–0.25 (MeV/amu)$^{1/2}$) are reasonably independent of ion type. Overall, it appears that corotating ion spectra at ~1–30 MeV/amu may be ordered by energy/amu or, equivalently, by ion speed. *Gloeckler et al.* [1979*a*, *b*] reported exponential in velocity distribution functions with $v_0 = 0.17 \pm 0.03$ (MeV)$^{1/2}$ at 0.3–10 MeV for protons, He, C, and O during the mid-1970s solar minimum, consistent with the present observations (though we note in passing

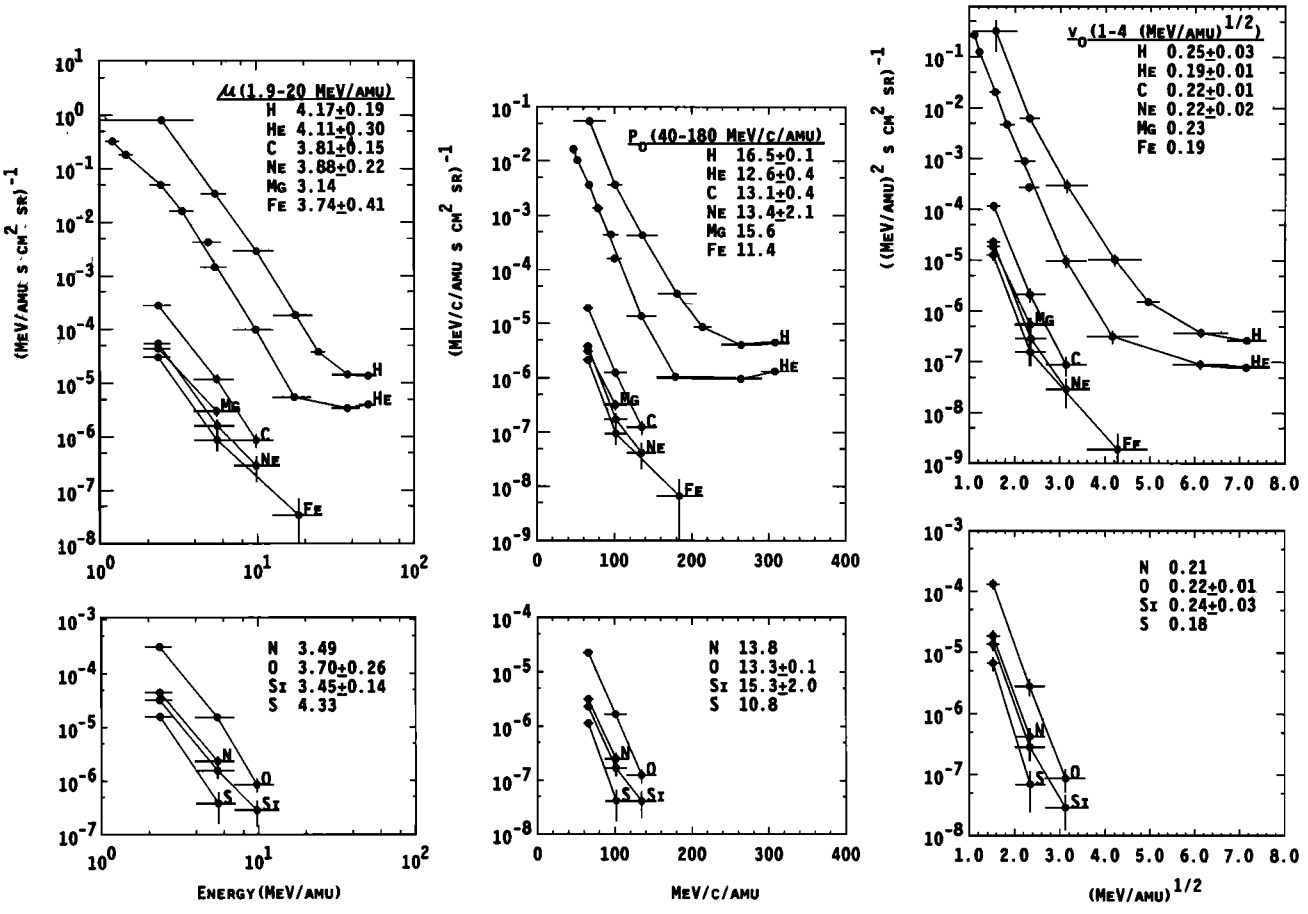

Fig. 12. Ion spectra summed over the corotating events during 1982–1986 in Table 1, plotted such that linear spectra represent power laws in energy, ($dJ/dE \approx E^{-\mu}$), exponentials in momentum ($dJ/dP \approx \exp(-P/P_0)$), and exponential in particle velocity distribution functions ($f \approx \exp(-v/v_0)$) in the left-hand, center, and right-hand panels, respectively.

that this form may not extend to lower (tens of keV) energies [*Richardson and Hynds*, 1990]).

To examine any solar cycle variation, spectra have been averaged over events in three time intervals: August 1978 to December 1981 (near solar maximum conditions), 1982 to 1983, and 1984 to 1986 (near solar minimum conditions). Figure 13 compares spectral indices obtained from 2 to 12 MeV/amu ion spectra for each time interval. (For clarity, the errors, which are generally less than ±0.5 and typically ±0.2, are not plotted.) The spectral indices are similar for all ion types and show little significant solar cycle dependence. Ion spectra have also been examined for each event by calculating spectral indices from the ratio of the 1.9–2.8 MeV/amu and 4–7 MeV/amu fluxes. Figure 14 indicates that the ^{4}He spectral index shows little correlation with either the event intensity (defined by the 1.1–1.34 MeV/amu ^{4}He intensity) or with the stream maximum solar wind speed. Figure 15 shows that spectral indices for various ions are generally correlated and comparable (as also indicated by Figure 8).

6.4. *Ion Abundances*

The spectra discussed above suggest that ion abundances may be compared at equal energy/amu. Table 2 shows ISEE 3/ICE 1.9–2.8 MeV/amu ion abundances (relative to oxygen) for corotating events in 1978–1981 (around solar maximum), 1982–1983, and 1984–1986 (near solar minimum). SEP abundances from the same instrument channel (obtained by *Cane et al.* [1991] from 36 events in September 1978 to April 1984)

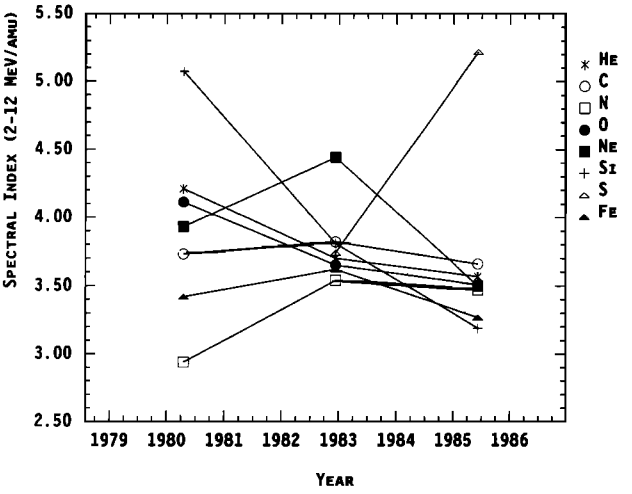

Fig. 13. Ion spectral indices for 2–12 MeV/amu ion spectra for 1978–1981, 1982–1983, and 1984–1986, showing little variation with solar cycle. Errors (not plotted) are <0.5 and typically ~0.2.

and SMCE abundances are also given. The corotating event abundances indicate a transition from ~SEP-like at solar maximum to SMCE-like at solar minimum. SEP contamination, or the acceleration of low-energy SEPs by corotating shocks at solar maximum, might be responsible though the lack of a solar cycle intensity dependence noted above suggests that this may not be the case. (*Shields et al.* [1985] noted a similar trend in the H/He abundance from solar minimum to solar maximum during the previous solar cycle during "nonflare, nonquiet" intervals which are expected to include corotating events, but attributed this to probable misidentification of some solar maximum intervals. Also the SEP-like Ne abundance at solar maximum suggests that impulsive flare events, which are Ne-rich [*Reames et al.*, 1990], do not contribute.) Alternatively, there may be a real systematic change between solar maximum and solar minimum corotating event abundances.

To investigate whether our measurements suggest a solar cycle abundance variation, Figure 16 shows that corotating streams were generally slower around the 1981 solar maximum than approaching solar minimum in 1982–1986, while the ^{4}He/O, proton/^{4}He (at 4–6 MeV/amu) and C/O ratios were generally more SEP-like (compare with Tables 2 and 3) around solar maximum and more SMCE-like elsewhere. While showing the solar cycle dependence, this raises the possibility that the abundance variations are related to the stream speed rather than simply to, for example, SEP contamination at solar maximum. An association between solar wind speed and corotating event composition was also suggested by Figure 8. In addition, *Marshall and Stone* [1978] noted a possible proton/^{4}He and solar wind speed anticorrelation, based on a small number of mid-1970s solar minimum events.

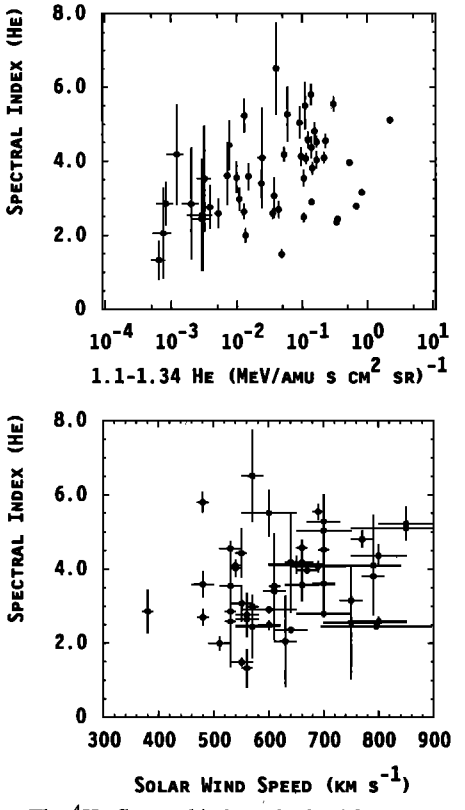

Fig. 14. The ^{4}He Spectral index, obtained from 1.9–2.8 and 4–7 MeV/amu intensities, shows only a weak correlation with the event size or the stream solar wind speed.

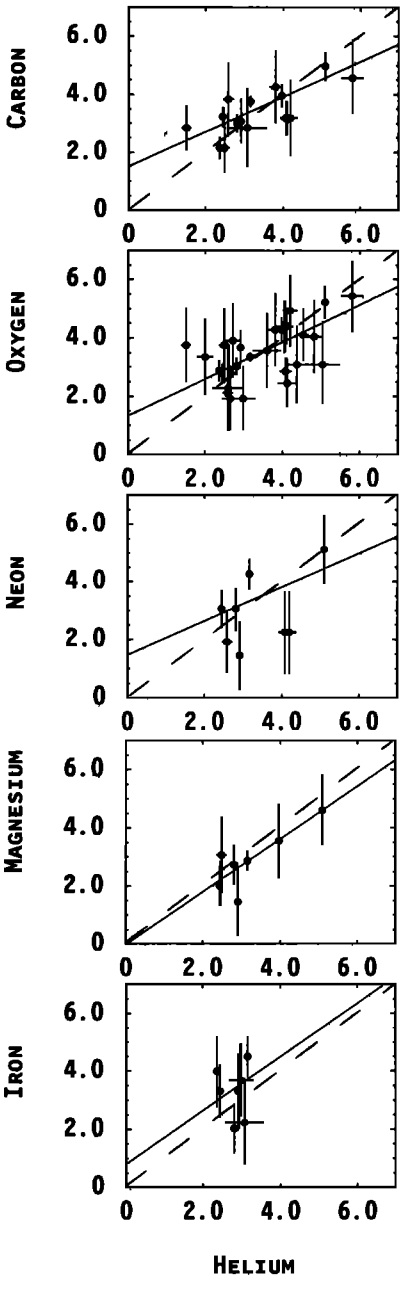

Fig. 15. Event-averaged ion spectral indices at 1.9–7 MeV/amu plotted versus the ^{4}He spectral index. The spectral indices show some correlation (a weighted least squares fit is indicated) and are approximately equal, the dashed lines indicating equal spectral indices.

The top panel of Figure 17 shows that an approximately linear correlation exists between the event-averaged ^{4}He/O ratios and the stream peak solar wind speed (both listed in Table 1). ^{4}He/O ranges from SEP-like values (~55) in lower speed (<600 km/s) streams to SMCE-like values (~150) in the faster (>700 km/s) streams. Many of the lower-speed streams are from solar maximum however, so SEP contamination might be responsible for this variation. To check this, the middle and bottom panels of Figure 17 show similar data

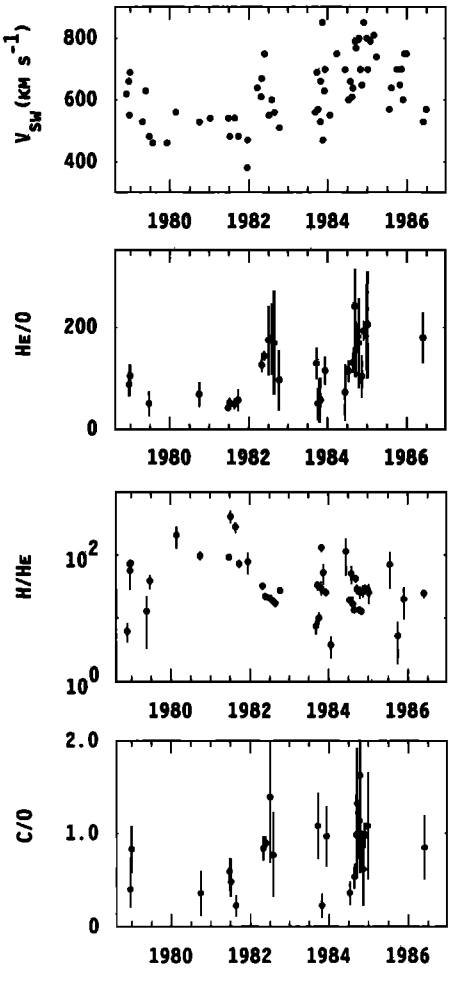

Fig. 16. The maximum solar wind speed and event-averaged H/^{4}He, ^{4}He/O, and C/O ratios for the streams in Table 1 plotted versus date of observation. Slower streams (which are more apparent around the 1981 solar maximum) are generally associated with more SEP-like abundances (see Table 2), and higher-speed streams are associated with SMCE-like abundances.

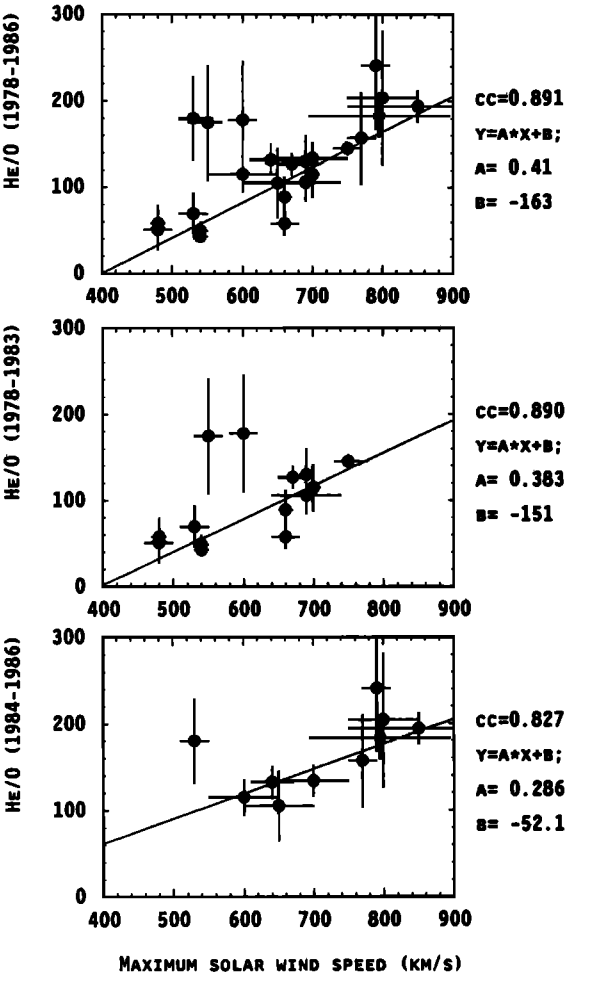

Fig. 17. Event-averaged ^{4}He/O abundance ratios plotted versus stream maximum solar wind speed for events in 1978–1986 (top panel), 1978–1983 (middle panel), and 1984–1986 (bottom panel). The positive correlations and similar linear fits to each group of events indicate that the abundance variations are not associated with changing solar activity levels but with solar wind speed.

TABLE 3. Abundances (O ≡ 1) for SEPs, Corotating Events in <600 km/s and >600 km/s Solar Wind Streams at 1.9–2.8 MeV/amu, and Solar Wind Plasma

	SEP[a]	<600 km/s	>600 km/s	SMCE[b]	Solar Wind[c]	High-Speed SW[c]
H	3700 ± 400[d]	2300 ± 200[e]	2500 ± 100[e]	2700 ± 200	1900 ± 400	945 ± 105[f]
^{4}He	55 ± 3	54 ± 23	130 ± 35	160 ± 50	75 ± 20	45 ± 5
C	0.48 ± 0.02	0.62 ± 0.06	0.89 ± 0.05	0.89 ± 0.1	···	0.529 ± 0.013
N	0.13 ± 0.01	0.15 ± 0.02	0.15 ± 0.01	0.14 ± 0.01	···	0.129 ± 0.008
Ne	0.15 ± 0.01	0.15 ± 0.02	0.17 ± 0.02	0.20 ± 0.04	0.17 ± 0.02	0.114 ± 0.008
Mg	0.21 ± 0.01	0.19 ± 0.03	0.14 ± 0.01	0.13 ± 0.03	···	0.106 ± 0.010
Si	0.15 ± 0.01	0.09 ± 0.02	0.11 ± 0.01	0.08 ± 0.02	0.19 ± 0.04	0.103 ± 0.011
S	0.035 ± 0.004	0.06 ± 0.02	0.05 ± 0.01	0.06 ± 0.01	···	0.038 ± 0.009
Fe	0.16 ± 0.02	0.14 ± 0.02	0.099 ± 0.01	0.096 ± 0.05	0.19 ± 0.07	0.124 ± 0.004
H/^{4}He	67 ± 10	43 ± 18	19 ± 5	17 ± 7	25 ± 8	21

[a] *Cane et al.* [1991].
[b] Solar minimum corotating events: *Gloeckler et al.* [1979*a*,*b*], *Scholer et al.* [1979], *McGuire et al.* [1978], *Christon and Simpson* [1979], and *von Rosenvinge and McGuire* [1985].
[c] *Gloeckler and Geiss* [1989].
[d] *McGuire et al.* [1986].
[e] H/He (4–6 MeV/amu) × He/O (1.9–2.8 MeV/amu).
[f] H/He (=21 [*Bame et al.*, 1977]) × He/O.

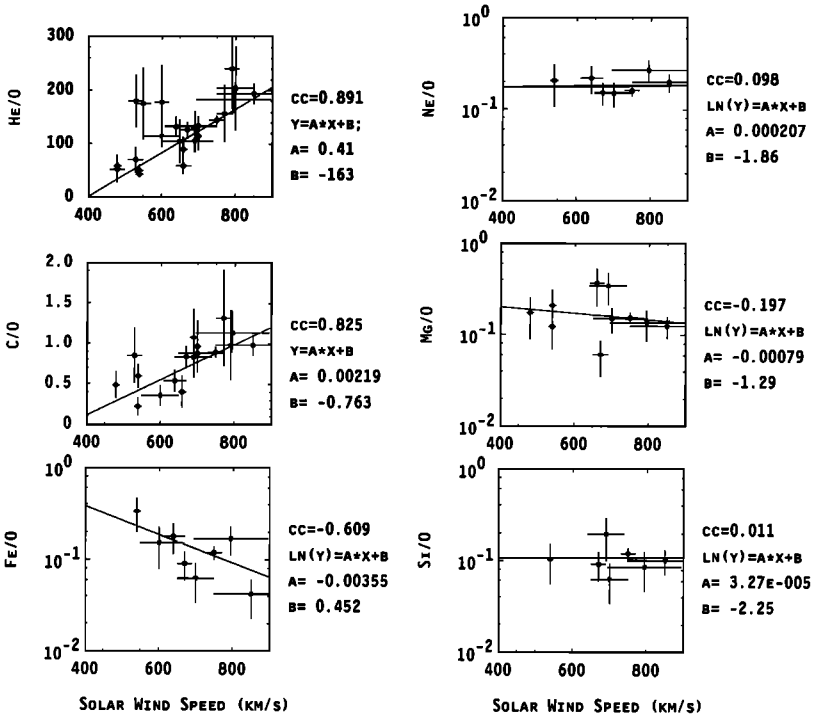

Fig. 18. Event-averaged corotating ion abundances relative to O versus stream solar wind speed. Where a trend is apparent, corotating event abundances tend to range from SEP-like at lower speeds (compare with Table 2) to SMCE-like in higher-speed streams.

for events in 1978 to 1983, around solar maximum, and in 1984 to 1986, near solar minimum conditions when SEP contamination should be considerably reduced. In each case, a positive correlation is apparent between ^{4}He/O and the stream solar wind speed. Furthermore, the lines fitted to each group of events are remarkably similar, with He/O $\approx$ 0.4 (V_{sw} (km/s)) − 150. This indicates that the ^{4}He/O ratio is dependent only on the solar wind speed and shows no solar activity dependence. Thus since SEP contamination does not appear to be significant, all events will be included in the subsequent analysis.

We now consider whether other ion abundances show correlations with solar wind speed. Figure 18 shows the solar wind speed versus event-averaged ^{4}He/O, C/O, Ne/O, Mg/O, Si/O, and Fe/O ratios. C/O and Fe/O ratios are also listed in Table 1. ^{4}He/O (as noted above) and C/O are clearly correlated with the solar wind speed, while Fe/O and possibly Mg/O are anticorrelated. Ne/O and Si/O show little trend. N/O, which also shows little trend, and S/O, where few measurements are available, are not plotted. Comparing Figure 18 with Table 2, where a trend is evident, this is consistent with a continuous transition from ~SEP-like abundances at slower speeds to ~SMCE-like at higher speeds. Figure 19 shows the event-to-event correlation between the ^{4}He/O and C/O ratios (top panel) and the anticorrelation between Fe/O and C/O (bottom panel), consistent with such a transition. The symbol size indicates the stream solar wind speed. Ion fluxes other than ^{4}He, C and Fe are generally insufficient to investigate solar wind speed-related abundance variations on an event-to-event basis. Thus the ion fluxes have been summed over all streams with solar wind speeds ≤600 km/s and >600 km/s. The resulting

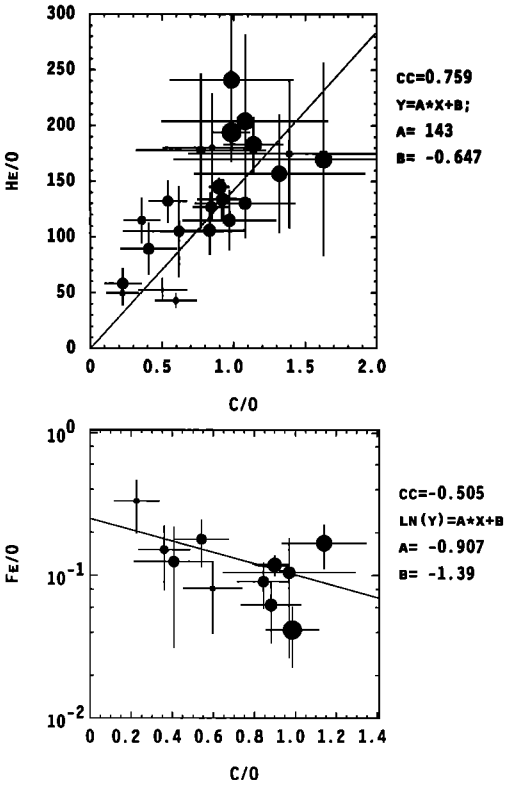

Fig. 19. Event-averaged C/O and ^{4}He/O (top panel), and C/O and Fe/O (bottom panel) ratios. The symbol size indicates the stream solar wind speed. The ratios show a continuous range of compositions from ~SEP-like at lower stream speeds to ~SMCE-like at higher speeds.

abundances relative to O are given in Table 3. Again there is a general transition from SEP-like abundances in lower speed streams to SMCE-like in faster streams.

If corotating events in high-speed streams are accelerated out of the solar wind plasma at corotating reverse shocks, abundance variations may be introduced by the acceleration process and subsequent propagation to 1 AU or may reflect variations in the high-speed stream plasma composition, for example, with changing solar wind speed. It is known that both SEP [*Meyer*, 1985*a*, *b*; *Breneman and Stone*, 1985] and SMCE abundances [*Reames et al.*, 1991; *Richardson et al.*, 1991] are ordered relative to photospheric abundances by the first ionization potential (FIP). Direct solar wind ion abundance measurements are summarized by *Gloeckler and Geiss* [1989] and included in Table 3. Although few observations have been made at high solar wind speeds (and these were made in the magnetosheath) and various important solar wind ion abundances have not yet been measured, solar wind plasma abundances also show evidence of a FIP dependence [*Meyer*, 1985*a*, *b*; *Gloeckler and Geiss*, 1989, and references therein]. A FIP dependence implies that abundances are determined in the upper chromosphere transition region [*Vauclair and Meyer*, 1985; *von Steiger and Geiss*, 1989; *Meyer*, 1991] where neutrals and ions coexist and FIP can influence ion abundances. (A FIP dependence is also shown by galactic cosmic ray abundances [*Meyer*, 1985*a*, *b*] possibly due to chromospheric fractionation in the source stars.) The energetic ion abundances in corotating events are presumably then ordered by FIP because of their origin in solar wind plasma. Corotating energetic ions may therefore be used as "proxies" to investigate coronal composition, augmenting direct solar wind composition measurements, as have SEP ions [e.g., *Breneman and Stone*, 1985; *Stone*, 1989].

The top panel of Figure 20 compares low speed solar wind plasma and SEP abundances (normalized to O) relative to photospheric abundances, plotted versus FIP. Corotating energetic particle (EP) event abundances for ≤600 km/s streams (from Table 3) are also plotted. There is reasonable agreement, with low-FIP ions overabundant by a factor of ~4 over photospheric values and depressed ^{4}He abundances. The low-FIP overabundance extends to ~11 eV, so that S is enhanced while C is only slightly so. H is anomalous in that it acts as a low-FIP element while having a FIP similar to that of O.

The bottom panel of Figure 20 compares SMCE, >600 km/s corotating stream energetic particle event and directly measured high-speed solar wind plasma abundances. All show a reduced low-FIP overabundance (~2.5) compared to the top panel. (Comparing with Figure 18 and Table 3, it is the low-FIP ion abundances which decrease with increasing solar wind speed.) However, the overabundance now extends above 11 eV and encompasses C, resulting in the increased C/O abundance at higher solar wind speeds. This is less clearly shown by the solar wind plasma, but the trend is evident. One difference between the compositions in Figure 20 is that ^{4}He is not depressed in high-speed stream-associated corotating events. This is also reflected by the increase in ^{4}He/O (Figure 17) and the increase in ^{4}He/(Mg+Si+Fe) (Figure 21) with solar wind speed. Also, H again acts as an overabundant, low-FIP ion in corotating events associated with >600 km/s streams even though the high-speed solar wind plasma H abundance (obtained by multiplying the ^{4}He abundance from *Gloeckler and Geiss* [1989] by H/^{4}He = 21 [*Bame et al.*, 1977]) is close to the photospheric value.

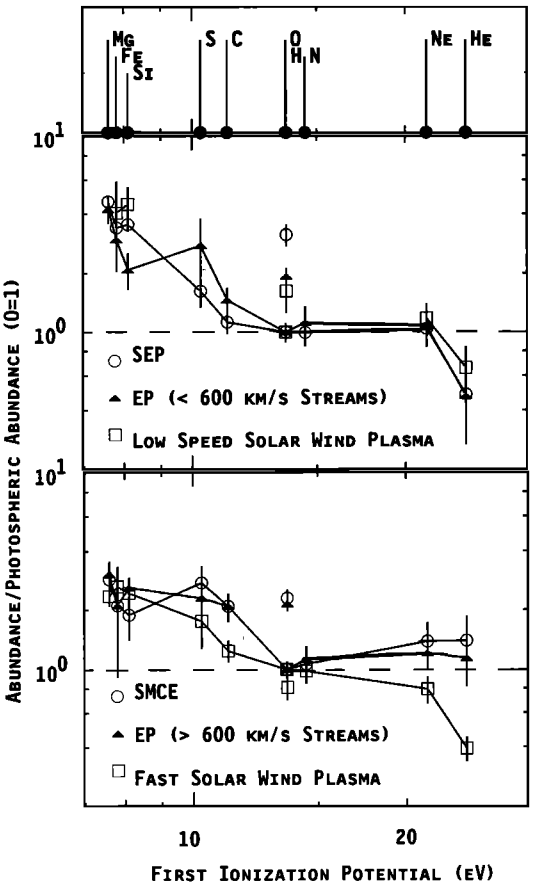

Fig. 20. (Top) Abundances (relative to O, from Table 3) for SEPs, energetic particles (EP) in <600 km/s corotating streams, and "low speed" solar wind plasma, divided by photospheric abundances and plotted versus first ionization potential (FIP). Oxygen ≡ 1 in each case and hence can be distinguished from hydrogen with nearly identical FIP. Elements with FIPs below ~11 eV are overabundant by a factor of ~4 in each case. ^{4}He is depressed below the photospheric abundance. H behaves as a low-FIP element. (Bottom) Similar data for solar minimum corotating events, energetic particles in >600 km/s corotating streams, and "high-speed" solar wind plasma. The low-FIP overabundance is now only a factor of ~2.5 but extends to ~12 eV so that C and S behave more like low-FIP ions than in the top panel. ^{4}He is not depressed in high-speed stream corotating events.

Thus with the exception of the H abundance (where the coronal and solar wind plasma abundances may also be in conflict [*Meyer*, 1991]) and within the limitations of present solar wind plasma composition measurements, corotating event abundances may reflect solar wind speed-associated changes in the plasma composition. We suggest that the different ~MeV/amu SEP and SMCE abundances arise from their origin in low- and high-speed solar wind plasma, respectively: SEP abundances are characteristic of low-speed solar wind presumably because travelling interplanetary shocks which accelerate these ions will more usually be propagating through lower-speed solar wind than through high-speed corotating streams. On the other hand, corotating events associated with high-speed streams are accelerated from high-speed stream plasma and hence reflect its composition. This also suggests that the composition of CIR

forward shock ion enhancements should be SEP-like since the ions are accelerated from low speed solar wind. This is consistent with the larger proton/^{4}He ratio (~100) at CIR forward shocks [*Barnes and Simpson*, 1976; *Hamilton et al.*, 1979] and implies that it may be difficult to distinguish between ions streaming sunward from CIR forward shocks and SEP decay phases based on their streaming and composition. Also, interplanetary shocks propagating through high-speed streams may be expected to accelerate SEPs with "SMCE-like" abundances.

The variable solar wind composition indicated by the energetic ions suggests that coronal composition is nonuniform and that conditions in the fractionation region in the chromosphere which determine the composition are associated with variations in the speed of the emitted solar wind. The temperature in the fractionation region may be greater below coronal holes, while the shorter residence time of gas in open field structures underlying coronal holes may lead to a weaker ion-neutral separation [*Meyer*, 1991], together accounting for the higher FIP threshold [*Feldman et al.*, 1990] and reduced low-FIP overabundance for high-speed solar wind and for energetic ions accelerated out of high-speed solar wind.

One final aspect to investigate is whether the difference between mean SEP and corotating event abundances is in fact dependent on the charge/mass (Q/A) ratio. A Q/A dependence may arise from particle acceleration and interplanetary propagation, which depend on ion rigidity and hence on Q/A [*Stone*, 1989]. In this case, the difference between corotating event and SEP abundances would be determined in interplanetary space and would not reflect changes in solar wind composition. The top panel of Figure 22 shows the ratio of mean SMCE and SEP abundances plotted versus Q/A and indicates that corotating event abundances are not ordered relative to mean SEP abundances by Q/A. In particular, Mg, Si, and Fe, which have similar FIPs but rather different Q/As, behave similarly in having reduced SMCE abundances relative to SEP abundances. We have adopted the Q/A values measured for SEPs by *Luhn et al.* [1985] here. However, the Q/A values may be lower in high-speed streams from coronal holes due to the lower

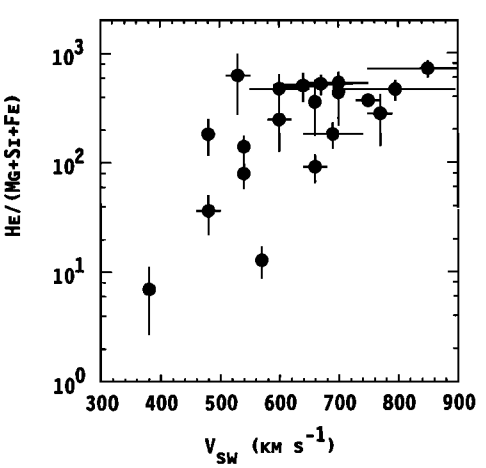

Fig. 21. The ^{4}He/(Mg+Si+Fe) ratio plotted versus stream solar wind speed. The increase with solar wind speed reflects the reduced overabundance of low-FIP ions and the smaller ^{4}He abundance depression.

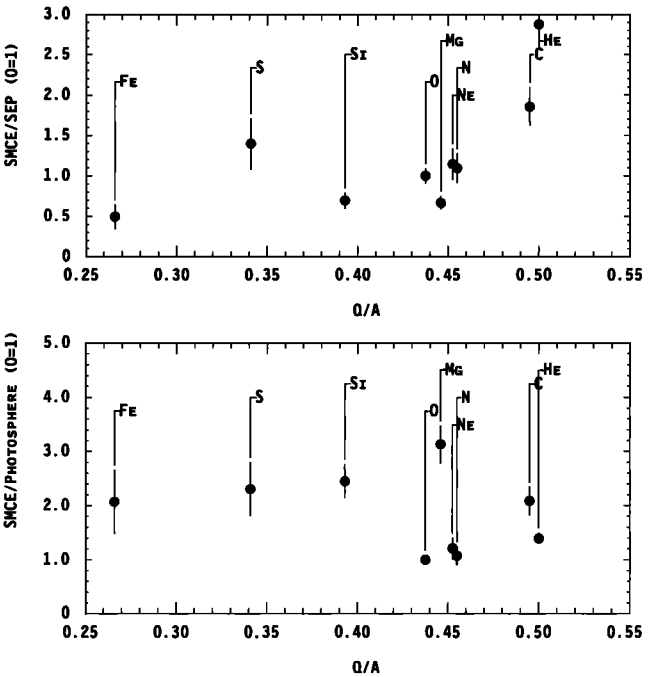

Fig. 22. (Top) Ratio of SMCE and mean SEP abundances as a function of Q/A. The difference between SMCE and mean SEP abundances is not ordered by Q/A. (Bottom) SMCE abundances relative to the photosphere, showing the absence of ordering by Q/A.

temperature in the lower corona where the ion charges are determined. *Arnauld and Rothenflug* [1985] have estimated the mean ion charge states as a function of plasma temperature (the *Luhn et al.* [1985] values apparently corresponding to temperatures of ~1.6–6.3 × 10^6 K). We have investigated whether the ion abundance ratios are better ordered by values of Q/A appropriate for lower temperature (>10^5 K) plasma but do not find any significant improvement. Overall, it appears that interplanetary acceleration and propagation conditions do not determine the abundance variations with respect to SEPs. The bottom panel of Figure 22 shows that SMCE abundances relative to the photosphere are also not ordered by Q/A. There is, however, a suggestion of a weak Q/A dependence, with a slightly higher abundance relative to the photosphere at higher Q/A, from comparing separately the low-FIP ions (Fe, S, Si, and Mg) and high-FIP ions (O, N, Ne, C, and He).

7. SUMMARY

The properties of ≥1 MeV/amu ions in 64 corotating high-speed streams observed in 1978–1986 at 1 AU have been investigated and found to be consistent with previous observations made generally during the mid-1970s solar minimum. Such streams were particularly evident during the decline from the 1981 solar maximum. Around 50% include significant ion intensity enhancements not associated with solar particle events or travelling interplanetary shocks. The ions stream nearly along the **E** × **B** drift direction in the spacecraft frame, corresponding to a weak ($A_1 \approx$ 5–40%) sunward, field-aligned streaming in the solar wind frame. The sunward streaming is consistent with particle acceleration in the outer heliosphere followed by diffusion into the inner heliosphere. Assuming a steady state diffusion-

convection propagation model, ~5–40% anisotropies combined with radial gradients of ~400%/AU imply field-aligned mean free paths of ~0.01–0.1 AU in high-speed streams, consistent with previous similar estimates. These mean free paths are considerably smaller than those (~1 AU) inferred from impulsive solar flare particle events [*Mason et al.*, 1989]. One possibility is that mean free paths are smaller in corotating high-speed streams due to, for example, the presence of large-amplitude Alfvén waves propagating away from the Sun [*Belcher and Davis*, 1971]. The impulsive events studied by *Mason et al.* [1989] were not observed in high-speed streams, so the existence of small mean-free paths in such streams is not necessarily ruled out by their observations. Alternatively, if mean-free paths in corotating streams are a large fraction of an AU, the diffusion-convection model and the conclusions inferred from it will be invalid. In this case, corotating ion enhancements may be set up by ion reflection between the corotating reverse shock and the increasingly intense magnetic fields closer to the Sun.

The ion intensity is not correlated with the stream solar wind speed or with the increase in solar wind speed at the leading edge of the high-speed stream, suggesting that the local shock strength alone may not play a dominant role in determining the intensity. Other effects may be important including the merging of CIRs in the outer heliosphere and the latitudinal extent of the CIR shocks since higher energies may, in general, be attained at more extended shocks. There is also no clear solar cycle dependence, suggesting that corotating events are not accelerated out of a background low energy SEP source population. A number of high-speed streams include low, near "quiet time", ion fluxes and may be observed on successive solar rotations. These "empty" streams may occur when two streams are closely spaced in heliolongitude and interact just beyond 1 AU, preventing the proper formation of corotating shocks (since the interaction is between two high-speed streams rather than between slow and high-speed solar wind) and accounting for the absence of accelerated ions. The ion intensity tends to fall at the stream interface, and increases at the trailing edge of the stream (Figure 10), suggesting that ambient ions in solar wind regions adjacent to the stream do not enter the stream, consistent with this being a large-scale plasma structure bounded by tangential discontinuities. Ion enhancements are generally absent at 1 AU in the slow solar wind preceding corotating high-speed streams, possibly due to the tendency for ion intensities to be lower at corotating forward shocks [*Barnes and Simpson*, 1976] (which may reflect the higher temperature of the plasma source at the reverse shock [e.g., *Scholer et al.*, 1980]), the longer path length along spiral field lines connecting to the forward shock compared to the reverse shock, and the more inhomogeneous nature of slow solar wind plasma which may inhibit particle propagation from the outer heliosphere. (On the other hand, the mean-free path may be longer than in high-speed streams, as noted above.)

The ion spectra at <1 MeV/amu to ~20 MeV/amu are ordered by energy/amu (i.e., by ion velocity) for the ions from protons to Fe investigated and are represented by a form which approximates to a power law in energy, $dJ/dE \approx E^{-\mu}$ with $\mu \approx 4$ above ~3 MeV/amu and $\mu \approx 2$–3 at lower energies. At >1 MeV/amu, this spectrum may be represented equivalently by an exponential in momentum $dJ/dP \approx \exp(-P/P_0)$, P_0 = 11–16 MeV/c/amu, or by a distribution function $f \approx \exp(v/v_0)$, v_0 = 0.18–0.25 (MeV/amu)$^{1/2}$. The spectra are essentially independent of the phase of the solar cycle and similar to those reported during the previous solar cycle at corotating reverse shocks in the outer heliosphere and at 1 AU.

Corotating event ion abundances are ordered relative to photospheric abundances by the first ionization potential and are correlated with stream solar wind speed, ranging from SEP-like abundances in slower (<600 km/s) streams to SMCE-like in higher speed streams. The abundances are not related to mean SEP abundances by Q/A and hence do not arise from the effects of interplanetary acceleration and propagation on a source population with SEP-like abundances. The solar wind speed-associated abundance changes may reflect variations in the solar wind plasma composition with solar wind speed (within the limitations of present solar wind composition measurements), consistent with ion acceleration from the solar wind. Mean SEP and high-speed stream-associated corotating event abundances may differ since interplanetary shocks, which accelerate SEPs, are more likely to be travelling through low speed solar wind than through corotating streams. (This will be particularly true during solar maximum when corotating streams are less prominent but SEP events are more frequent.) Also, the different compositions of energetic ion enhancements at corotating forward and reverse shocks in the outer heliosphere may be due to their acceleration from slow and high-speed solar wind, respectively. The ordering of energetic ion and solar wind plasma abundances relative to photospheric abundances by first ionization potential indicates that the ion abundances are related to conditions in the fractionation region of the upper chromosphere. In particular, the temperature of the fractionation region may be higher, and the ion-neutral separation weaker, below coronal holes from which higher speed solar wind is emitted.

Acknowledgments. We thank J.-P. Meyer for useful discussions.

The Editor thanks S. Christon and another referee for their assistance in evaluating this paper.

REFERENCES

Armstrong, T. P., G. Chen, E. T. Sarris, and S. M. Krimigis, Acceleration and modulation of electrons and ions by propagating interplanetary shocks, in *Study of Travelling Interplanetary Phenomena*, edited by M. A. Shea et al., p. 367, D. Reidel, Hingham, Mass., 1977.

Arnauld, M., and R. Rothenflug, An updated evaluation of recombination and ionization rates, *Astron. Astrophys. Suppl.*, *60*, 425, 1985.

Bame, S. J., J. R. Asbridge, W. C. Feldman, and J. T. Gosling, Evidence for a structure-free state at high solar wind speeds, *J. Geophys. Res.*, *82*, 1487, 1977.

Barnes, C. W., and J. A. Simpson, Evidence for interplanetary acceleration of nucleons in corotating interaction regions, *Astrophys. J. Lett.*, *210*, L91, 1976.

Belcher, J. W., and L. Davis, Large amplitude Alfvén waves in the interplanetary medium, 2, *J. Geophys. Res.*, *76*, 3534, 1971.

Breneman, H. H., and E. C. Stone, Solar coronal and photospheric abundances from solar energetic particle measurements, *Astrophys. J.*, *299*, L57, 1985.

Bryant, D. A., T. L. Cline, U. Desai, and F. B. McDonald, Continual acceleration of solar protons in the MeV range, *Phys. Rev. Lett.*, *14*, 481, 1965.

Burlaga, L. F., Interplanetary stream interfaces, *J. Geophys. Res.*, *79*, 3717, 1974.

Cane, H. V., D. V. Reames, and T. T. von Rosenvinge, Solar particle abundances at energies of greater than 1 MeV per nucleon and the role of interplanetary shocks, *Astrophys. J.*, *373*, 675, 1991.

Chao, J. K., V. Formisano, and P. C. Hedgecock, Shock pair observation, in Solar Wind, edited by C. P. Sonett, P. J. Coleman, Jr., and J. M. Wilcox, *NASA Spec. Publ.*, *SP-308*, 435, 1972.

Christon, S. P., On the origin of the MeV energy nucleon flux associated with CIRs, *J. Geophys. Res.*, *86*, 8852, 1981.

Christon, S. P., Energetic interplanetary nucleon flux anisotropies: The effect of Earth's bow shock and magnetosheath in sunward flow, *J. Geophys. Res.*, *87*, 5045, 1982.

Christon, S. P., and J. A. Simpson, Separation of corotating nucleon fluxes from solar flare fluxes by radial gradients and nuclear composition, *Astrophys. J. Lett.*, *227*, L49, 1979.

Couzens, D. A., and J. H. King, Interplanetary medium data book, Supplement 3, 1977–85, NSSDC/WDCA, Goddard Space Flight Cent., Greenbelt, Md., 1986.

Decker, R. B., M. E. Pesses, and S. M. Krimigis, Shock associated low energy ion enhancements observed by Voyagers 1 and 2, *J. Geophys. Res.*, *86*, 8819, 1981.

Dryer, M., Interplanetary shock waves: Recent developments, *Space Sci. Rev.*, *17*, 277, 1975.

Feldman, U., K. G. Widing, and P. A. Lund, On the anomalous abundances of the 2×10^4-2×10^5 K solar atmosphere above a sunspot, *Astrophys. J.*, *364*, L21, 1990.

Fisk, L. A., On the acceleration of energetic particles in the interplanetary medium, *J. Geophys. Res.*, *81*, 4641, 1976.

Fisk, L. A., and M. Lee, Shock acceleration of energetic particles in corotating interaction regions in the solar wind, *Astrophys. J.*, *237*, 620, 1980.

Gloeckler, G., and J. Geiss, The abundance of elements and isotopes in the solar wind, in Cosmic Abundances of Matter, *AIP Conf. Proc.*, *183*, 49, 1989.

Gloeckler, G., D. Hovestadt, F. M. Ipavich, and G. M. Mason, Distribution function representation of energy spectra of H, He, C, O and Fe in corotating particle streams, *Proc. Int. Cosmic Ray Conf. 16th*, *5*, 368, 1979*a*.

Gloeckler, G., D. Hovestadt, and L. A. Fisk, Observed distribution functions of H, He, C, O, and Fe in corotating energetic particle streams: Implications for interplanetary acceleration and propagation, *Astrophys. J.*, *230*, L191, 1979*b*.

Gold, R. E., C. O. Bostrom, E. C. Roelof, and D. J. Williams, Anisotropy measurements of ~50 keV solar protons, *Proc. Int. Cosmic Ray Conf. 14th*, *5*, 1801, 1975.

Hamilton, D. C., G. Gloeckler, T. P. Armstrong, W. I. Axford, C. O. Bostrom, C. Y. Fan, S. M. Krimigis, and L. J. Lanzerotti, Recurrent energetic particle events associated with forward/reverse shock pairs near 4 AU in 1978, *Proc. Int. Cosmic Ray Conf. 16th*, *5*, 363, 1979.

Hundhausen, A., *Coronal Expansion and Solar Wind*, Springer-Verlag, New York, 1972.

Hundhausen, A., Solar activity and the solar wind, *Rev. Geophys.*, *17*, 2034, 1979.

Joselyn, J. A., and P. S. McIntosh, Disappearing solar filaments: A useful predictor of geomagnetic activity, *J. Geophys. Res.*, *86*, 4555, 1981.

Kunow, H., G. Wibberenz, G. Green, R. Muller-Mellin, M. Witte, H. Hempe, R. Mewaldt, E. Stone, and R. Vogt, Simultaneous observations of cosmic ray particles in a corotating interplanetary structure at different solar distances between 0.3 and 1 AU, *Proc. Int. Cosmic Ray Conf. 15th*, *3*, 227, 1977.

Lindbald, B. A., H. Lundstedt, and B. Larsson, A third catalogue of high-speed plasma streams in the solar wind-data for 1978–1982, *Sol. Phys.*, *120*, 145, 1989.

Logachev, Yu. I., V. G. Stolpovskii, M. A. Zel'dovich, A. J. Somogyi, K. Kecskeméty, M. Tátrallyay, A. Varga, K. I. Gringauz, M. I. Verigin, and I. N. Klimenko, Recurrent enhancements of energetic particle intensity during the decreasing phase of 21st solar activity cycle, *Proc. Int. Cosmic Ray Conf. 21st*, *5*, 320, 1990.

Luhn, A., D. Hovestadt, B. Klecker, M. Scholer, G. Gloeckler, F. M. Ipavich, A. B. Galvin, C. Y. Fan, and L. A. Fisk, The mean ionic charges of N, Ne, Mg, Si, and S in solar energetic particle events, *Proc. Int. Cosmic Ray Conf. 19th*, *4*, 241, 1985.

Marshall, F., and E. C. Stone, Characteristics of sunward flowing protons and alpha particle fluxes of moderate intensity, *J. Geophys. Res.*, *83*, 3289, 1978.

Mason, G. M., C. K. Ng, B. Klecker, and G. Green, Impulsive acceleration and scatter-free transport of ~1 MeV per nucleon ions in ^{3}He-rich solar particle events, *Astrophys. J.*, *339*, 529, 1989.

McDonald, F. B., and U. Desai, Recurrent solar cosmic ray events and solar M regions, *J. Geophys. Res.*, *76*, 808, 1971.

McDonald, F. B., B. J. Teegarten, J. H. Trainor, T. T. von Rosenvinge, and W. R. Webber, The interplanetary acceleration of energetic nucleons, *Astrophys. J. Lett.*, *203*, L149, 1976.

McGuire, R. E., T. T. von Rosenvinge, and F. B. McDonald, The composition of corotating energetic particle streams, *Astrophys. J. Lett.*, *224*, L87, 1978.

McGuire, R. E., T. T. von Rosenvinge, and F. B. McDonald, The composition of solar energetic particles, *Astrophys. J.*, *301*, 938, 1986.

Mewaldt, R. A., E. C. Stone, and R. E. Vogt, The radial diffusion coefficient of 1.3–2.3 MeV protons in recurrent proton streams, *Geophys. Res. Lett.*, *5*, 965, 1978.

Meyer, J.-P., The baseline composition of solar energetic particles, *Astrophys. J. Suppl.*, *57*, 151, 1985*a*.

Meyer, J.-P., Solar-stellar outer atmospheres and energetic particles, and galactic cosmic rays, *Astrophys. J. Suppl.*, *57*, 173, 1985*b*.

Meyer, J.-P., Diagnostic methods for coronal abundances, *Adv. Space Res.*, *11*(1), 269, 1991.

Neugebauer, M., and C. W. Snyder, Mariner 2 observations of the solar wind, 1, Average properties, *J. Geophys. Res.*, *71*, 4469, 1966.

Palmer, I. D., and J. T. Gosling, Shock-associated energetic proton events at large heliocentric distances, *J. Geophys. Res.*, *83*, 2037, 1978.

Perez-Enriquez, R., and B. Mendoza, Low latitude coronal hole as the only possible explanation for the November 25, 1978, geomagnetic storm, *J. Geophys. Res.*, *95*, 10,717, 1990.

Pesses, M. E., J. A. Van Allen, and C. K. Goertz, Energetic protons associated with interplanetary active regions 1–5 AU from the Sun, *J. Geophys. Res.*, *83*, 553, 1978.

Pesses, M. E., B. T. Tsurutani, J. A. Van Allen, and E. J. Smith, Acceleration of energetic protons by interplanetary shocks, *J. Geophys. Res.*, *84*, 7297, 1979.

Reames, D. V., H. V. Cane, and T. T. von Rosenvinge, Energetic particle abundances in solar electron events, *Astrophys. J.*, *357*, 259, 1990.

Reames, D. V., I. G. Richardson, and L. M. Barbier, On the differences in element abundances of energetic ions from corotating events and from large solar events, *Astrophys. J. Lett.*, *382*, L43, 1991.

Richardson, I. G., Spacecraft observations at 1 AU of low energy ions in co-rotating solar wind streams, Ph.D. thesis, Univ. of London, 1983.

Richardson, I. G., Anisotropy of >35 keV ions in corotating particle events at 1 AU, *Planet. Space Sci.*, *33*, 147, 1985*a*.

Richardson, I. G., Low energy ions in co-rotating interaction regions at 1 AU: Evidence for statistical ion acceleration, *Planet. Space Sci.*, *33*, 557, 1985*b*.

Richardson, I. G., and R. J. Hynds, Low energy (>35 keV) proton enhancements associated with co-rotating solar wind streams at 1 AU, *Proc. Int. Cosmic Ray Conf. 17th*, *3*, 430, 1981.

Richardson, I. G., and R. J. Hynds, Spectra of >35 keV ions in corotating ion enhancements at 1 AU: ISEE-3/ICE observations, *Proc. Int. Cosmic Ray Conf. 21st*, *5*, 337, 1990.

Richardson, I. G., and R. D. Zwickl, Low energy ions in corotating interaction regions at 1 AU: Observations, *Planet. Space Sci.*, *32*, 1179, 1984.

Richardson, I. G., D. V. Reames, K.-P. Wenzel, and J. Rodriguez-Pacheco, Quiet-time properties of low energy (<10 MeV/amu) interplanetary ions during solar maximum and solar minimum, *Astrophys. J.*, *363*, L9, 1990.

Richardson, I. G., D. V. Reames, L. M. Barbier, and T. T. von Rosenvinge, MeV/n ions associated with corotating high-speed

solar wind streams at ≤1 AU during 1978 to 1986, *Proc. Int. Cosmic Ray Conf. 22nd*, *3*, 288, 1991.

Sanahuja, B., V. Domingo, K. P. Wenzel, J. A. Joselyn, and E. Keppler, A large proton event associated with solar filament activity, *Sol. Phys.*, *84*, 321, 1983.

Scholer, M., D. Hovestadt, B. Klecker, and G. Gloeckler, The composition of energetic particles in corotating events, *Astrophys. J.*, *227*, 323, 1979.

Scholer, M., G. Morfill, and M. A. I. Van Hollebeke, On the origin of corotating energetic particle events, *J. Geophys. Res.*, *85*, 1743, 1980.

Shields, J. C., T. P. Armstrong, S. P. Eckes, and P. R. Briggs, Solar and interplanetary ions at 2–4 MeV/nucleon during solar cycle 21: Systematic variations of H/He and He/CNO ratios and intensities, *J. Geophys. Res.*, *90*, 9439, 1985.

Smith, E. J., and J. Wolfe, Pioneer 10, 11 observations of evolving solar wind streams and shocks beyond 1 AU, in *Study of Travelling Interplanetary Phenomena*, edited by M. A. Shea et al., p. 227, D. Reidel, Hingham, Mass., 1977.

Snyder, C. W., and M. Neugebauer, The relation of Mariner-2 plasma data to solar phenomena, in *The Solar Wind*, edited by R. J. Mackin and M. Neugebauer, p. 25, Pergamon, New York, 1966.

Stilwell, D. E., R. M. Joyce, B. J. Teegarten, J. H. Trainor, G. Streeter, and J. Bernstein, The Pioneer 10/11 and Helios A/B cosmic ray instruments, *IEEE Trans. Nucl. Sci.*, *NS-22*, 570, 1975.

Stone, E. C., Solar abundances as derived from solar energetic particles, in Cosmic Abundances of Matter, *AIP Conf. Proc.*, *183*, 72, 1989.

Tang, F., B. T. Tsurutani, W. D. Gonzalez, S. I. Akasofu, and E. J. Smith, Solar sources of interplanetary southward B_z events responsible for major magnetic storms (1978–1979), *J. Geophys. Res.*, *94*, 3535, 1989.

van Hollebeke, M. A. I., F. B. McDonald, and T. T. von Rosenvinge, The radial variation of corotating energetic particle streams in the inner and outer solar system, *J. Geophys. Res.*, *83*, 4723, 1978.

van Hollebeke, M. A. I., F. B. McDonald, J. H. Trainor, and T. T. von Rosenvinge, Corotating energetic particles and fast plasma streams in the inner and outer solar system in radial dependence and energy spectra, in *Solar Wind Four*, edited by H. Rosenbauer, p. 497, Max-Planck-Institut für Extraterrestrische Physik, Garching, Germany, 1979.

Vauclair, S., and J.-P. Meyer, Diffusion in the chromosphere, and the composition of the solar corona and energetic particles, *Proc. Int. Cosmic Ray Conf. 19th*, *4*, 233, 1985.

von Rosenvinge, T. T., and R. E. McGuire, Elemental abundances in corotating events, *Proc. Int. Cosmic Ray Conf. 19th*, *9*, 547, 1985.

von Rosenvinge, T. T., F. B. McDonald, J. H. Trainor, M. A. I. Van Hollebeke, and L. A. Fisk, The medium energy cosmic ray experiment for ISEE-C, *IEEE Trans. Geosci. Electr.*, *GE-16*(3), 208, 1978.

von Rosenvinge, T. T., J. C. Brandt, and R. W. Farquhar, The International Cometary Explorer mission to comet Giacobini-Zinner, *Science*, *232*, 353, 1986.

von Steiger, R., and J. Geiss, Supply of fractionated gases to the corona, *Astron. Astrophys.*, *225*, 222, 1989.

Whang, Y. C., Shock interactions in the outer heliosphere, *Space Sci. Rev.*, *57*, 339, 1991.

Wilcox, J. M., and N. F. Ness, Quasi-stationary corotating structure in the interplanetary medium, *J. Geophys. Res.*, *70*, 5793, 1965.

Zel'dovich, M. A., Yu. I. Logachev, S. P. Ryumin, and V. G. Stolpovskii, The spectra of 30–750 keV protons in the recurrent particles fluxes according to the "Prognoz-4, 5" measurements, *Proc. Int. Cosmic Ray Conf. 17th*, *3*, 422, 1981.

Zwickl, R. D., and E. C. Roelof, Interplanetary propagation of <1 MeV protons in nonimpulsive energetic particle events, *J. Geophys. Res.*, *86*, 5449, 1981.

Zwickl, R. D., and W. R. Webber, Limitations of the COS approximation as applied to the cosmic ray anisotropy, *Nucl. Instrum. Methods*, *138*, 191, 1976.

L. M. Barbier, D. V. Reames, I. G. Richardson, and T. T. von Rosenvinge, Code 661, Laboratory for High Energy Astrophysics, NASA Goddard Space Flight Center, Greenbelt, MD 20771.

(Received December 30, 1991;
revised June 22, 1992;
accepted July 27, 1992.)